University of Stavanger

Faculty of Science and Technology

MASTER'S THESIS

Study program/ Specialization: Biological chemistry	Spring semester, 2017 Open
Writer: Sumit Gautam	……
Faculty Supervisor: Lutz Andreas Eichacker External Supervisor: Johannes Lange	
Title of master's thesis: **"ANALYSIS OF CELLULAR EVENTS IN A CELL MODEL FOR NEURODEGENERATIVE DISEASES INVOLVING MITOCHONDRIAL DAMAGE"**	
Credits (ECTS): 60	
Key words: Mitochondrial isolation Gel electrophoresis 6-OHDA cytotoxicity Immunofluorescence microscopy	Pages: …68…… + supplementary materials: …5 …… Stavanger,…09.06.17……..

UNIVERSITY OF STAVANGER

ANALYSIS OF CELLULAR EVENTS IN A CELL MODEL FOR NEURODEGENERATIVE DISEASES INVOLVING MITOCHONDRIAL DAMAGE

BY

SUMIT GAUTAM

A thesis submitted in partial fulfillment for the degree of Master of Science in Biological Chemistry

In the Department of Mathematics and Natural Science

Faculty of Science and Technology

Faculty Supervisor: Lutz Andreas Eichacker

External Supervisor: Johannes Lange

09 June 2017

Declaration of Authorship

I, SUMIT GAUTAM, declare that this thesis entitled **"ANALYSIS OF CELLULAR EVENTS IN A CELL MODEL FOR NEURODEGENERATIVE DISEASES INVOLVING MITOCHONDRIAL DAMAGE"** and the work presented in it are my own. I confirm that:

- This work was done wholly or mainly while in candidature for a research degree at this University.
- Where any part of this thesis has previously been submitted for a degree or any other qualification at this University or any other institution, this has been clearly stated.
- Where I have quoted from the work of others, the source is always given. With the exception of such quotations, this thesis is entirely my own work.
- Where I have consulted the published work of others, this is always clearly attributed.
- I have acknowledged all main sources of help.
- Where the thesis is based on work done by myself jointly with others, I have made clear exactly what was done by others and what I have contributed myself.

Signed: ……

Date……June 9,2017…….

ACKNOWLEDGEMENT

I would like to express my deepest gratitude and appreciation to my supervisor, Prof. Dr. Lutz Andreas Eichacker and Co-supervisor Dr. Johannes Lange, for their excellent guidance and patience during my Master's one year thesis at the University of Stavanger. It was a fantastic opportunity to work under their supervision over the last several months. Beside the research, I got valuable time and ideas in learning the good lab techniques which, undoubtedly, will be helpful for me in the days to come. Their enthusiasm and curiosity toward science provided me with a colossal atmosphere and motivation to work on the project. They were both energetic and excited about the project and supportive when I needed assistance, especially when it came to areas in which I had inadequate knowledge and experience. I am truly grateful for all the time, generosity, support and the opportunities, they gave me during the whole project.

A big thank you goes to all the people of the Lutz lab and cell lab for their incredible support, help, discussions and guidance. Thanks to Xiang Ming as well, who provided the training in Confocal Laser Scanning Microscope. Finally, I would like to thank friends and colleagues while I was studying at UiS and working on the thesis at CORE.

ABSTRACT

Mitochondria are highly dynamic organelles, with an essential role in proper cell function. Increasing evidence points towards a key role of mitochondria and its bioenergetic state for pathogenesis of neurodegenerative diseases like Parkinson´s disease. Nonetheless, the study of defects in mitochondrial dynamics has been linked with a better understanding of the pathophysiology of such an enigmatic disease. Here, the isolation of pure mitochondria from neuronal cells was investigated, since it is a crucial step to perform proteomics research on the organelle, which can be helpful in exploring the intricate role of mitochondria in neurodegeneration. In addition, the influence of 6-OHDA, proven to have cytotoxic action in neuronal cells has been tested, since the precise underlying mechanism is unknown.

Several mitochondria isolation and extraction methods were tested. Dounce homogenization technique has been found to be the most promising technique and was pursued further to improve the protocol and isolate the mitochondria from neuroblastoma cells, SHSY5Y. Moreover, the cytotoxic effect of neurotoxin 6-OHDA on SHSY5Y cells, was investigated using the XTT assay method, to find the concentration for 6-OHDA that impairs, but not kills the cells (aiming at 50% survival). The effect of 6-OHDA on different proteins of neuronal cells like TOM20, MAP2, IL-6Rα and alpha-synuclein were studied using immunofluorescence microscopy. Here, the cytotoxic effect of 6-OHDA on cell viability in SHSY5Y cells were reproduced. Interestingly, this neurotoxin was also found likely to have detrimental effects on mitochondrial proteins like TOM20, microtubular protein MAP2, IL-6Rα and alpha-synuclein. We discuss that 6OHDA can directly or indirectly affect the neuronal cells which might lead to cell death. The underlying mechanism behind the effects of 6-OHDA on the cell proteins remained elusive. Further detailed studies of 6-OHDA action on neuronal cell should be performed on the molecular level to develop an appropriate therapeutic strategy for the neurodegenerative diseases.

ABBREVIATIONS

PD	Parkinson's Disease
SN	Substantia Nigra
MAO	Monoamine Oxidase
NMDA	N-methyl-D-aspartate receptor
COMT	Catechol-O-methyltransferase
DDI	DOPA decarboxylase inhibitor
UPS	Ubiquitin proteasome system
PARK	Parkin
AD	Autosomal Dominant
AR	Autosomal Recessive
ROS	Reactive Oxygen Species
IMM	Inner mitochondrial membrane
IMS	Intermembrane space
OMM	Outer mitochondrial membrane
NADH	Nicotinamide-adenine dinucleotide
ADP	Adenosine diphosphate
ATP	Adenosine triphosphate
MPTP	1-Methyl-4-Phenyl-1,2,3,6-tetrahydropyridine
SNP	Single Nucleotide Polymorphism
SOD	Superoxide Dismutase
Fe	Iron
H_2O_2	Hydrogen Peroxide

DA	Dopamine/Dopaminergic
SNc	Substantia nigra pars compacta
L-DOPA	Dihydroxyphenylalanine
6-OHDA	6 Hydroxydopamine
NO	Nitric oxide
ECACC	European Collection of Authenticated Cell Cultures
BCA	Bicinchoninic acid assay
BN PAGE	Blue Native Polyacrylamide Gel Electrophoresis
SDS PAGE	Sodium Dodecyl Sulfate Polyacrylamide Gel Electrophoresis
RT	Room temperature
MTS	Mitochondrial Targeting Signal
GP	Glycoprotein
DH	Dounce homogenization
MIK	Mitochondrial isolation kit
iNOS	Inducible Nitric Oxide synthase
TOM	Translocase of outer mitochondrial membrane
PINK1	PTEN induced putative kinase 1
MTS	Mitochondrial targeting sequence
MAP	Microtubule-associated protein
MT	Microtubule
IL6R	Interleukin 6 receptor
Sil6R	Soluble interleukin 6 receptor

TABLE OF CONTENTS

LIST OF TABLES

LIST OF FIGURES

1. INTRODUCTION

1.1 Parkinson's disease

Parkinson's disease (PD) is a chronic and the second most neurodegenerative disease after Alzheimer's disease, which affects up to 4 % of the population over age 80 in Western Europe (Lau & Breteler, 2006), and with a prevalence of about 1% in people over the age of 60 (Lau & Breteler, 2006; Xie, Hu, & Li, 2010). Several studies have evinced the sharp increase in the onset of PD after the age of 60, with the most likely occurrence in male than in female (Lau & Breteler, 2006). PD is typified by the cardinal motor symptoms like bradykinesia, rigidity and uncontrollable tremor which are the upshots of the death of dopamine- (DA-) producing neurons of the substantia nigra (SN) and the resultant depletion of DA in the striatum (Hornykiewicz, 1998). PD, the most prevalent neurodegenerative disorder, is hallmarked by the depigmented SN and the presence of filamentous rich alpha-synuclein inclusions as Lewy bodies in SN and other brain regions (Braak et al., 2000).

To date, there is no cure for PD nor a therapy that can halt the disease. All treatment is symptomatic and most patients experience a decreased efficacy for drug treatment. Drug side effects like induced impulse control disorders complicate the picture (Müller, 2012). According to Muller et al. 2012, among all the drugs tested, levodopa has been established as the most efficacious and best endurable drug for motor symptom control since long. Levodopa, when given concomitantly with Catechol-O-methyltransferase (COMT) and DOPA decarboxylase inhibitor (DDI) increases its half-life and efficacy which substantially reduces the motor symptoms but the onset of motor complications in the advanced stage of PD has been a noticeable predicament. The onset of motor complications is believed to occur, because of fluctuations of dopamine concentration in the brain, loss of presynaptic dopaminergic autoreceptor functions, compensating abilities to avoid high dopamine concentration in the synaptic cleft and induction of frequent alternating irregular postsynaptic dopamine receptor stimulation. The complications like wearing off and dyskinesia resulting from the use of levodopa, as also described by Muller et al. 2012, lead to the convoluted treatment schedules in the later stage which could indicate the failure of drug therapy (AH Schapira, 2008).

Importantly, the lack of knowledge for the exact neuronal loss mechanism extant in such disease has led to the discovery of only symptomatic relief treatments with not any prominent cure till today. The disease progression is almost impossible to halt as the neuronal loss is a rapid process

(Dexter & Jenner, 2013). As such, research has been carried out using an in-vitro neuronal cell model to understand the exact underlying pathogenesis of PD which can give a preeminent idea to develop an effective therapeutic strategy (Xie et al., 2010).

PD cases are predominantly idiopathic and in 5-10% of the cases arise from genetic causes that can follow both a recessive and dominant mode of inheritance (Wood-Kaczmar, Gandhi, & Wood, 2006). Moreover, Wood-Kaczmar et al. 2006, also avowed the numerous factors including mitochondrial dysfunction, oxidative stress, protein phosphorylation, protein misfolding and Ubiquitin-dependent proteasomal system (UPS) impairment in both inherited and sporadic form of PD. Their implementation in the disease process must be essentially considered with the characterization of proteins in the normal physiological and diseased state.

1.1.1 Genetic and environmental causes

Different gene mutations and the environmental factors have been supposed to damage the dopaminergic cell selectively in SN in PD. Various twin and family studies as well as the mapping and cloning of parkin (PARK) genes pertinent to PD, has been substantial to establish the genetic factor, a possible risk factor for PD. However, the exact underlying mechanism is still unknown (Warner & Schapira, 2003).

PARK-PD related genes along with their clinical features and inheritance mode are listed in Table 1.1.

Table 1.1: Overview of the most common PARK loci (adapted from (Klein & Westenberger, 2012; Warner & Schapira, 2003))

Locus	Inheritance	Gene	Status and remarks	Number of families	Clinical features	Reference
PARK1	AD	SNCA	confirmed	13	Early onset, rapid progression	(Polymeropoulos, Lavedan, Leroy, & Ide, 1997)
PARK2	AR	Parkin	confirmed	>60	Juvenile onset, dystonia	(Kitada, Asakawa, Hattori, & Matsumine, 1998)
PARK3	AR	Unknown	unconfirmed	6	Late onset PD	(Gasser, 2004)
PARK4	AD	SNCA	Erroneous loci identical to PARK1	1	Early onset, dementia, postural tremor	(Farrer et al., 1999)
PARK5	AD	UCH-L1	unconfirmed	1	Typical PD	(Leroy, Boyer, Auburger, Leube, & Ulm, 1998)
PARK6	AR	PINK1	confirmed	9	Early late onset, slow progression	(Mouradian, 2002)
PARK7	AR	DJ-1	confirmed	2	Early onset	(Bonifati, Rizzu, Baren, & Schaap, 2003)
PARK8	AD	LRRK2	confirmed	1	Typical PD	(Funayama, Hasegawa, Kowa, & Saito, 2002)

Among the different PARK associated genes responsible for PD, the gene encoding alpha-synuclein has been the center of attraction to study pathogenesis of PD. Several lines of evidence have depicted that the fibrillary, beta pleated sheet conformation of alpha-synuclein as well as its overexpression are highly responsible for the neurodegeneration (Steece-Collier, Maries, & Kordower, 2002). The accumulation of alpha-synuclein which is mostly localized to the presynaptic terminal in a neuron, has been supposed to be involved in PD through its

oligomerization and fibrillar growth. However, the exact relevance of alpha-synuclein for PD hasn't been deciphered at the molecular level yet (Lashuel, Overk, & Oueslati, 2013).

Findings of neuropathological changes that were involved in the degeneration of dopaminergic neuron were also found to be related to various neurotoxicants (pesticides like manganese, MPTP) and neuroprotective compounds (tobacco products) on the nigrostriatum which depicts the relation between the environment and PD. These compounds likely produce the neurochemical and pathological features of idiopathic parkinsonism comprising the neurodegeneration, possibly through a myriad of events and interactions with the endogenous elements (Monte, Lavasani, & Manning-Bog, 2002).

Beside the exclusive roles of gene and environment as a risk factor for Parkinson's disease, several studies have elucidated the interplay between genes and the environmental factors as the next possible causative factor for Parkinson's susceptibility (Gao & Hong, 2011). Hui Ming et al. 2011 asserted that several Single Nucleotide polymorphism (SNP) in multiple genes, with the exposure to various herbal pesticides like paraquat and heavy solvents can augment the risk of PD susceptibility. Moreover, according to Collier et al. al. 2002, neuronal cell death can be promoted through the enhanced oligomerization of alpha-synuclein by iron, copper, nucleation and increased ROS induced by neurotoxins like 1-Methyl-4-Phenyl-1,2,3,6-tetrahydropyridine (MPTP) which likely illustrates the role of an interconnection between the gene and environmental factors for causing PD.

1.2 SHSY5Y as a cellular model

The SHSY5Y, a human neuroblastoma cell line with many features of dopaminergic neurons, is a thrice cloned cell line SK-N-SH established originally from a neuroblastoma patient (Biedler, Helson, & Spengler, 1973). The expression of tyrosine and dopamine β-hydroxylases, as well as dopamine transporter in such cells, regulates the synthesis of dopamine and noradrenaline and dopamine homeostasis, respectively. These cell lines bear biochemical and functional neuronal properties due to which it has been extensively used as the cell model for the neuronal disease since long (Xie et al., 2010). Moreover, Xie et al. 2010, asserted that the highly proliferating nature of these cell lines during the cell culture in the long run has met the requirement for an in-vitro cell model. As SHSY5Y cell mimic many features of Dopaminergic (DA) neuronal cell death when treated with the various neurotoxins, this cell has become the most commonly used cell type in the neurodegenerative research field with the aim to unveil the mechanism involved in selective loss of DAergic neurons in SN (Xie et al., 2010).

1.3 Mitochondria and cellular oxidative stress

1.3.1 Mitochondria

Mitochondria, synonymously the powerhouses of the cell, are the semiautonomous organelles enclosed by a double membrane. The organelle comprises of three compartments as the outer mitochondrial membrane (OMM), the intermembrane space (IMS) and the inner mitochondrial membrane (IMM). The IMM forms cristae and the mitochondrial matrix (Murray & Kincaid, 2012). The presence of the pore-forming membrane proteins (porins) in OMM helps in the transport of small uncharged molecules while the larger molecules pass across the membrane with the support of special translocases only. On the other hand, the particular molecules and ions are able to pass across the inner membrane only with the help of specific membrane transport proteins, that ultimately engender the membrane potential of about 180 mV across IMM (Kühlbrandt, 2015).

1.3.2 Electron Transport Chain

Primarily, mitochondria are the main energy source of the cell. Different multisubunit enzyme complexes, located in the inner mitochondrial membrane are actively involved in ATP synthesis through the process called oxidative phosphorylation. In this process, the free energy in respiratory chain substrates is transformed into an electrochemical potential across the IMM. While electrons reduce molecular oxygen, protons are concentrated in the IMS and utilized for ATP production in the matrix (Sazanov, 2015).

Electrons and protons are from redox carrier molecules are used in the electron transport chain, by five integral membrane protein lipid enzyme complexes including complex I which accepts $NADH+H^+$ from the mitochondrial matrix, reduces ubiquinone and transfers protons to the IMS. Complex II directly connects the respiratory chain to the metabolic citric acid cycle and used $FADH_2$ for reduction of the membrane integral ubiquinone pool. Complex III uses reduced ubiquinone to reduce cytochrome c in the IMS and concomitantly pumps protons into the IMS; while complex IV uses the electron from cytochrome c for the reduction of molecular oxygen resulting in the formation of water at the matrix side of the IMM. Finally, also complex IV contributes to the transfer of protons to the IMS and the storage of energy in the potential difference between the IMS and the mitochondrial matrix which can be released by complex V to synthesize ATP from ADP (Figure 1.1).

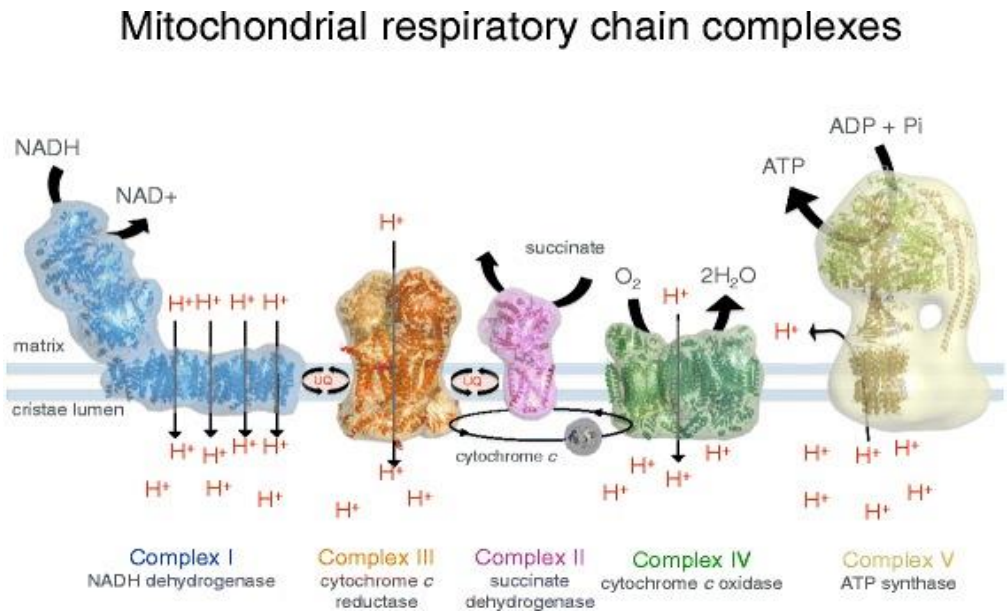

Figure 1.1: Membrane protein complexes of the respiratory chain. Electron transport complexes I (NADH/ubiquinone oxidoreductase, blue), II (succinate dehydrogenase, pink), III (cytochrome c reductase, orange), IV (cytochrome c oxidase, green) and the mitochondrial ATP synthase (also known as complex V, tan) work together in oxidative phosphorylation to harness energy for the cell. Complexes I, III and IV pump protons across the cristae membrane, creating the proton gradient that drives ATP synthesis. UQ ubiquinol (Davies & Daum, 2013).

The five complexes embedded in the IMM require not only a coordination of 85 protein subunits for concerted electron and proton transfer regulation but also are of dual genetic origin. Out of the 85 subunits, 72 are encoded by nuclear DNA, while 13 are encoded by mitochondrial DNA (mtDNA) which requires a sophisticated regulation of their expression, protein transport and assembly to establish and maintain operation of the ETC (AHV Schapira, 2007) (Table 1.2).

Table 1.2: The respiratory chain and oxidative phosphorylation system (adapted from (AHV Schapira, 2007))

Complex	**No. of subunits**	**MtDNA - encoded subunits**
Complex I	43	7
Complex II	4	-
Complex III	11	1
Complex IV	13	3
Complex V	14	2

1.3.3 Oxidative stress

The oxidative Phosphorylation system in mitochondria is imperative for ATP synthesis (Fig. 1.1); however, especially the reduction of oxygen is a critical step in this system and can lead to the production of superoxide radicals termed reactive oxygen species (ROS) (Liu, Fiskum, & Schubert, 2002; AHV Schapira, 2007). ROS are highly reactive oxygen molecules including the superoxide, and hydroxyl radical, and hydrogen peroxide.

A cellular antioxidant system prevails in the cells, capable of evicting ROS in a way to maintain the normal physiological state. Highly reactive O_2^- is inactivated by Superoxide Dismutase (SOD) to less reactive hydrogen peroxide which can be subsequently removed by enzymes like glutathione peroxidase, catalase and peroxiredoxins. It is of central importance that the activity level of the antioxidant system is found to be reduced in the Substantia nigra pars compacta (SNc) of PD (Kim, Kim, Rhie, & Yoon, 2015). While the superoxide radicals which may evade from the imperfect antioxidant system can damage the protein, lipid and DNA directly, hydroxyl radicals generated from the less reactive hydrogen peroxide cause a lipid peroxidation of the membrane. This ultimately causes cellular damage, termed oxidative stress (Brand, Affourtit, Esteves, & Green, 2004).

1.3.4 Mitochondrial dysfunction and oxidative stress

The dynamic nature of mitochondria as cell organelles, associated with its normal fusion, fission, turnover and subcellular recruitment, regulates mitochondrial function. The impairment in mitochondrial dysfunction can result in the establishment of a neurological disease like PD in which the depletion of ATP production as well as the increase in ROS result in bioenergetic failure (Henchcliffe & Beal, 2008; Perier & Vila, 2012). Especially, the autoxidizing capacity of dopamine to yield ROS at normal pH results in mitochondrial dysfunction, if not eliminated by the intracellular arsenal of antioxidants. The net level of ROS then keeps on escalating because of abating capability of antioxidants to scavenge deleterious free oxygen radicals (Lotharius & Brundin, 2002).

A. B.

Figure 1.2: A. Dopamine B.L-DOPA (Tsunoda, 2006)

The production of free radicals during dopamine synthesis via the deleterious dopamine quinone formation (Falkenburger & Saridaki, 2016) and the significantly increased level of iron in degenerating substantia nigra (Riederer, Sofic, & Rausch, 1989) are the striking evidences for the neurodegeneration in PD. According to Riederer et.al. 1989, the innocuous hydrogen peroxide gets rapidly decomposed to hydroxyl radicals in the presence of an iron complex and iron proteins like ferritin, thereby resulting the loss of membrane integrity and fluidity. The oxidative stress caused due to the mitochondrial dysfunction therefore, is a major risk factor for PD (Lin & Beal, 2006).

1.4 6-OHDA

6-OHDA is a structural analog of catecholamine, dopamine and noradrenaline. It was the first of the discovered neurotoxins that has been successfully used for modeling PD in experimented animals (Simola, Morelli, & Carta, 2007). Numerous studies reviewed the outrageous effects of 6-OHDA, a prototypical “oxidative stress neurotoxin”, on catecholaminergic pathways in rodents as well as on various cultured cell types (Przedborski & Ischiropoulos, 2005). Interestingly, having a peculiar effect on quantifiable circling motor disorders in an animal has made the unilateral 6-OHDA rat model a successful preclinical PD model to assess the antiparkinsonian effects (Tieu, 2011). The detection of the higher concentrations of endogenous 6-OHDA in urine samples of patients with PD than in those of normal patients elucidates the etiology of this toxin in PD which has created a basic foundation for the potential drug therapy development (Duty & Jenner, 2011; Jellinger, Linert, Kienzl, Herlinger, & Youdim, 1995).

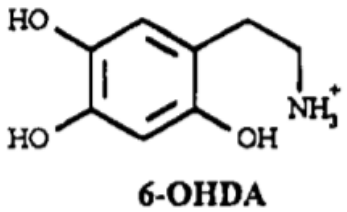

6-OHDA

Figure 1.3: Structure of 6-OHDA (Napolitano, Crescenzi, & Pezzella, 1995)

6-OHDA, having the higher affinity to catecholaminergic neuron, gets accumulated in the cytosol after its reuptake by dopaminergic and noradrenergic transporter molecules. This eventually causes cell death with no apoptotic feature (Schober, 2004). The oxidation of 6-OHDA in the brain by Monoamine Oxidase (MAO-A) and its auto-oxidation, both are significantly responsible for neuronal cell damage. The neuronal cell is then damaged because of the oxidation products (Reactive Oxygen Species) of 6-OHDA (Simola et al., 2007). This statement is strongly corroborated by Blum et al. 2001, who also emphasized the role of elevated iron level, in addition to MAO- A and auto-oxidation products, for ROS production (Figure 1.4).

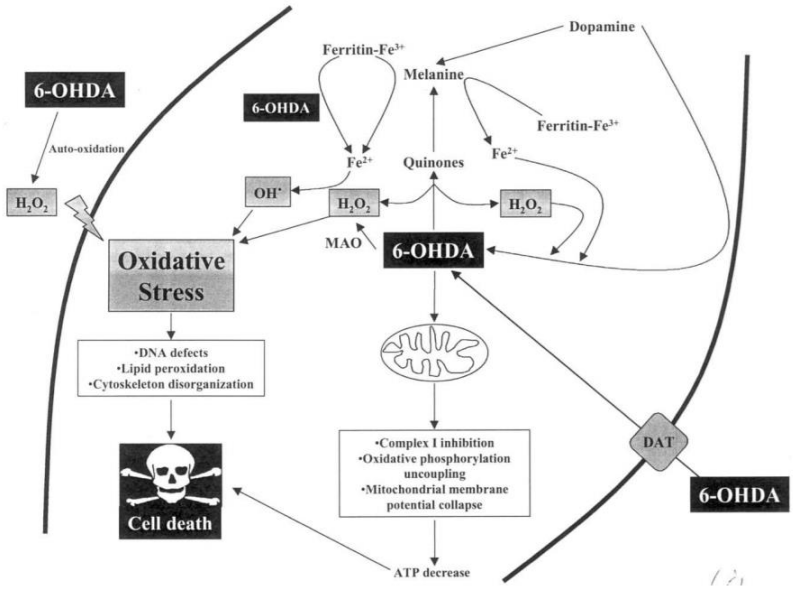

Figure 1.4: Hypothetical mechanism of 6-OHDA toxicity. 6-OHDA could induce catecholaminergic cell death by three main mechanisms: reactive oxygen species generated by intra or extracellular auto-oxidation, hydrogen peroxide formation induced by Monoamine oxidase (MAO) activity or direct inhibition of the mitochondrial respiratory chain. These events lead to strong oxidative stress amplified by cytoplasmic free calcium and to a decrease in cellular ATP availability, both leading to cell death (adapted from (Blum, Torch, Lambeng, & Nissou, 2001)).

The ultimate oxidation products of 6-OHDA have also been described to cause cell death through DNA strand break, mutations, disorganization of the cytoskeleton and impairment of glucose and alpha aminoisobutyric acid uptake (Blum et al., 2001). Apart from this, Blum et al. 2001 asserted also that 6-OHDA toxicity resulting in significant alteration in mitochondrial membrane potential as well as defect in dopamine vesiculation are highly associated with the mitochondrial impairment, thereby causing cell death.

The majority of scientific studies has suggested that the ROS produced by 6-OHDA in SHSY5Y cells, causes in particular apoptotic cell death, not only by decreasing the mitochondrial membrane potential with high intracellular calcium and subsequent release of cytochrome c, but also by translocation of NF- kB that induces nitric oxide synthase and intracellular NO release (Song et al., 2010). On the contrary, Sun et al., 2016 recently asserted that 6-OHDA at higher concentrations, in particular more than 250 µM, and upon incubation for 1 hr., causes a significant increase in mitochondrial membrane potential along with intracellular calcium overload eventually causing necrotic cell death in SHSY5Y neuroblastoma cells. This suggested that 6-OHDA can induce protease activated apoptosis at lower concentrations, while

protease inhibited accidental cell necrosis at higher concentrations (Kroemer, Dallaporta, & Resche-Rigon, 1998).

Astonishingly, it is also revealed that ROS produced after the oxidation of 6-OHDA contributes mitochondrial fragmentation in neuronal SHSY5Y cells while the use of aged 6-OHDA (6-OHDA stock solution aged for 1 month) and incubation of the cells with antioxidants like catalase and ascorbic acid failed to induce mitochondrial fission (Gomez-Lazaro, Bonekamp, & Galindo, 2008).

1.5 OBJECTIVES

Neurodegenerative diseases like PD, have gained wide attention because of lack of proper therapy and cure. The study of neuronal cells can play a pivotal role in developing a therapeutic strategy for the disease. The project was carried out in neuronal cell, SHSY5Y, to get the better insight into the pathogenesis of PD. The major objectives of the project were:

- Isolate intact mitochondria from the neuroblastoma cell line SHSY5Y cell for subsequent analysis
- use the isolated mitochondria and SHSY5Y cells for analysis of 6-OHDA on cell viability
- Study the effect of 6-OHDA on different proteins in SHSY5Y cells

2. MATERIALS AND METHODS

2.1 MATERIALS

2.1.1 Cell line

The dopaminergic human neuroblastoma cell line, SHSY5Y was used in this study.

Cell line	**Cat#**
SHSY5Y	ECACC

2.1.2 Homogenizer

Homogenization is a preliminary process of releasing the cell organelles and other cell constituents by breaking the plasma membrane gently so that the it results 90% of cell breakage reproducibly. Generally, under mildest condition, homogenization in aqueous media is highly preferred for the effective yield of homogenates (de Araújo, Lamberti, & Huber, 2015; Graham, 2002). Syringe based cell homogenizer (Isobiotech) and Dounced homogenizer (Dounce tissue grinder, Sigma-Aldrich, cat# D8938-SET) were used to homogenize the cells in our study.

2.1.3 Kits

Table 2.1: Different kits list

Material	**Manufacturer**	**Catalog number**	**Use**
Mitochondrial isolation Kit i. Reagent A- 50 ml ii.Reagent B- 0.5 ml iii.Reagent C- 65 ml	Thermoscientific	Lot# RG235588	Mitochondrial isolation
Cell Proliferation kit XTT i. XTT reagent – (10 × 5 ml) ii. Activation reagent – (2× 0.5 ml)	Applichem	1330140	Quantitating of cell proliferation

2.1.4 Reagents

The various reagents used are enlisted in table 2.2.

Table 2.2: Reagents used in experiments

Material	**Manufacturer**	**Catalog number**	**Use**
DMEM	GE health care	SH30081.01	Cell culture
L glutamine 200 mM	GE health care	SH30034	Cell culture
Phosphate buffer saline tablet	Gibco-life technology	1713582	Cell culture
Fetal Bovine serum	Life technology	10099-141	Cell culture
Protease inhibitor	ROCHE	04693159001	Cell culture
Penicillin/Streptomycin	GE health care	SV30010	Cell culture
Trypsin EDTA 10x	GE health care	SV30037.01	Cell culture
Non-essential amino acid 100x	Biowest	XO557-100	Cell culture
DPBS	GE heath care	SH30028.02	Cell culture
Super signal west Dura Luminar Enhancer solution	Thermoscientific	QE216025	Western blot
Super signal west Dura stable peroxide buffer	Thermoscientific	QE216025	Western blot
Roti block 10x	Carl ROTH	A151.1	Western blot
6-OHDA	Sigma Aldrich	H116	Enhancing cell toxicity
Seeblue Plus2 Prestained standard	Invitrogen Thermofischer scientific	LC 5925	SDS PAGE
Unstained protein marker	Invitrogen novex life technology	1819931	BN PAGE

2.1.5 Antibodies

The various antibodies used are enlisted below in table 2.3 and 2.4.

Table 2.3: List of antibodies used in this study with specific dilutions and applications

	Name	**Manufacturer**	**Source**	**concentration**	**Application**
Primary antibody	COXIV (3EII) MAb	Cell Signalling technology	Rabbit	1:1250	Western blot
Secondary antibody	NA934V	GE Health care alpha	Rabbit	1:50000	Western blot

Table 2.4: Preparation of primary and secondary antibodies for staining

Antibodies		**Dilution with blocking solution**	**Supplier**
1.Primary antibodies	Set I: Rabbit anti TOMM 20 alexa 488	1:100	abcam
	Mouse anti MAP 2	1:25	Santa Cruz
	Set II: Alpha SNCA	1:50	Santa Cruz
	IL-6Rα(C-20):sc661	1:25	Santa Cruz
2.Secondary antibodies	Set I: Anti mouse Alexa 568	1:400	Life technology
	Set II: Anti mouse (goat) alexa 568	1:400	Life technology
	Anti-rabbit (goat) alexa 488	1:400	Life technology

2.1.6 Prepared solutions and antibodies

1x PBS, 1L (gibco, cat 1713582)

- 1 PBS tablet
- 1000 ml MilliQ water

Various buffers prepared for cell homogenization, BN PAGE and SDS PAGE during the experiment are as follows:

Table 2.5: Buffer recipe for homogenization

Homogenization buffer	**Stabilization buffer**	**Maintainance buffer**
10 mM Tricine 5 mM NaCl pH adjusted to 7.4 with Bis-Tris	10 mM Tricine 5 mM NaCl 525 mM mannitol 175 mM sucrose pH adjusted to 7.4 with Bis-Tris	10 mM Tricine 5 mM NaCl 210 mM mannitol 70 mM sucrose pH adjusted to 7.4 with Bis-Tris

Table 2.6: Buffer recipe for BN PAGE

Concentrations 1x Running buffer (1L)	**Weigh in gram for 1x**	**Concentration 6x gel buffer**	**Weight in gm for 6x in 100ml**
50 mM $BisTris^{+}$, 50 mM Tricine-, 80 µM LDS pH 7.4	6.057 8.95	357 mM Bis Tris 205 mM HCl PH 6.5	44.8

Table 2.7: 10x TMK buffer recipe

Components	**Stock**	**dilution**	**End concentration**	**Total(ml)**
Tris HCl pH6.8	1M	1:10	100 mM	10
$MgCl_2$	1M	1:10	100 mM	10
KCl	2M	1:10	200 mM	10
				Upto 100 with 70 ml water

Table 2.8: Buffer recipe for SDS PAGE

system	Concentration 1x running buffer(1ltr)	Weight in gm for 1x	Concentration 6x gel buffer	Weight in gm for 6x in 100ml
Bis/MES	50 mM Tris 50 mM MES 1 mM EDTA 0.1% SDS 2mMSodium bisulfite pH 7.1	6.057 9.76 0.37	357 mM Bis Tris 205 mM HCl PH 6.5	44.8

Table 2.9: Loading buffer recipe for SDS

2x loading buffer
0.5 M Tris HCl, - PH 6.8 Glycerol 100% -2 ml Bromophenol blue - 0.02 gm SDS - 0.4 gm Making the final volume upto 9.6 ml with water Add 0.4 ml DTT just before loading

Table 2.10: Composition to cast SDS mini gels in the BioRad gel-tank

	Separation gel 12.5%(for 4 gels)	Stacking gel 4%(for 4 gels)
Distilled Water (ml)	14.7	4
Gel buffer 6x (ml)	4.2	1
Acrylamide (ml)	6.24	0.8
TEMED (µl)	44	20.5
APS (µl)	88	40.6
Total (ml)	25.272	5.861

The transfer buffer required for western blotting was made, as enlisted below.

Table 2.11: Transfer buffer recipe

Transfer buffer (75 ml)
Methanol- 7.5 ml
20x NUPAGE buffer NP0006- 3.75 ml
Make volume upto 75 ml with distilled water

2.2 METHODS

2.2.1 Cell culture

2.2.1.1 Dopaminergic human neuroblastoma cell line SHSY5Y

All SHSY5Y cell lines were grown in DMEM (45 ml high glucose) supplemented with 10% (v/v) Foetal Bovine serum heat inactivated (FBS), penicillin or streptomycin (10000U/ml or 10000µg/ml respectively;100 times the stock), L-glutamine (200mM) and non-essential amino acids (by Biowest). The cells were grown in 75 cm^2 flask in a humidified cell incubator at 37° C under 5% CO_2 atmosphere. The SHSY5Y cell lines were used upto passage number 27.

2.2.1.2 Aseptic technique

The aseptic technique was strictly followed during cell culture and their harvest. They were exclusively done in a dedicated cell culture room, negatively pressurized relative to the adjoining staging area, and requiring use of gowns and shoe covers for further protection. Hands were washed properly before wearing the nitrile gloves. The gloves were also sterilized with 70% ethanol solution. The work was carried out inside the laminar flow hood which was also sterilized with the ethanol solution before and after using it. All the reagents, bottles, solutions were sterilized before placing them in the hood. The equipments were handled with proper care to avoid any contamination from non-sterile surface as well as any breakage of the equipments. Any bacterial or other contaminations were closely checked in the cell cultures.

2.2.1.3 Rescuscitation of frozen culture

The cryotube containing the cell stock was thawed in a 37°C water bath for about 2 minutes (min). The cell content was then transferred to the cell culture flask containing DMEM medium (10 ml). The flask was incubated in a humidified cell incubator at 37°C and at 5% CO_2.

2.2.1.4 Sub-culturing

Sub-culturing was performed upon the cells reaching 80-90% confluence. Upon reaching this confluency, the medium DMEM from the cell culture flask was carefully aspirated without disturbing the adherent cells on the bottom of flask. The cells in the flask was washed with the warm sterile DPBS (10 ml PBS) which rinse any serum from the cells. The PBS was then removed. Subsequently, the cells were then digested with the mixture of 0.25% trypsin and warm DPBS for about 3 min in a humidified cell incubator at 37°C with 5% CO_2 until the majority of cells were detached. The trypsin reaction with the cells was stopped by adding 5 ml warm DMEM to the flask with cells. The cells were collected after rinsing the cells by pipetting

up and down several times to ensure a suspension of single cells. The collected cell suspension was centrifuged for about 5 min at 9 × 100 rpm at room temperature. The supernatant was discarded carefully and the obtained pellet was resuspended in 1 ml fresh warm DMEM. A small definite portion of cell suspension was pipetted into new 75 cm^2 flask containing 10 ml fresh DMEM, which was then incubated in a humidified cell incubator at 37°C with 5% CO_2.

2.2.1.5 Harvesting and counting of cells

The cells were harvested after the cells were about 90% confluent. The cells in the flask were harvested as described above and the obtained cell pellet was resuspended in 1 ml fresh warm DMEM media. 10 µl of cell suspension, from the mixture of 5 µl of cell suspension and 95 µl of DMEM, was pipetted under the slide cover of the Burker counting chamber to count the cell number. The equation to calculate the cell per ml is given by:

Cell/ml = Cell Count × dilution fator × 10^4, where Count = Average cells per 4 × 4 (1 mm) square

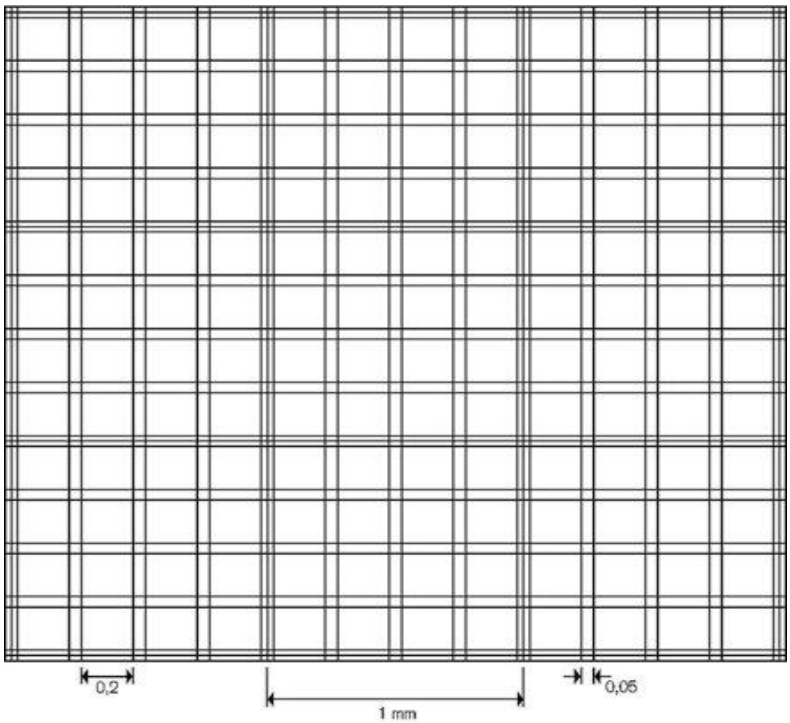

Figure 2.1: Burker counting chamber (Layout and dimensions) (Image: Sigma Aldrich)

2.2.2Mitochondrial isolation

After initial testing, the homogenization with the Dounce tissue grinder gave the best results; thus inspired, this method was used for the subsequent experiments.

2.2.2.1 Cell harvest

1. **Trypsination method**:

Cells were grown in 175 cm^2 flasks to 80-90% confluency and detached using 0.25% trypsin as described above. However, after centrifugation of the harvested cells, the pellet was washed with ice-cold PBS and centrifuged again at 900 rpm (100 × g). The supernatant was discarded carefully and the cell pellet was washed with cold PBS and centrifuged again under the same conditions. The cell pellet was resuspended in cold homogenization buffer (Table 2.5) with protease inhibitors – (at least 5x more buffer than pellet was added). The cell sample (ranging from 3.5 $\times 10^7$ to 7×10^7 cells) were kept on ice for further procedures.

2. **Scraping method**

However, for the cells grown in 75 cm^2 flask, scraping method was used instead of trypsination of cells. Firstly, after the cells were about 80-90% confluent, the cells were washed twice with the ice cold sterile PBS. The cells were then subsequently washed with the homogenization buffer (10 mM Tricine, 5 mM NaCl, pH adjusted to 7.4 with Bis-Tris. The homogenization buffer was aspirated as much as possible and the cells were scraped off with a cell lifter (3-5x on each spot is suffice). The cells were collected and 1/50 volume of 50x protease inhibitor was added to the collected cells. The cells were kept on ice and taken for mitochondrial isolation by homogenization and subsequent differential centrifugation.

2.2.2.2 Homogenization

The cell sample was homogenized using two methods as described below:

A. Dounce Cell homogenization (keep everything on ice)

The cells were homogenized with slow and gentle strokes in the douncer using pestle A for 3 min (douncer is still on ice, about 24 strokes). The homogenization was continued with pestle B for 3-5 min (still on ice, about 30 strokes). The cell sample was collected and centrifuged at 800 × g for 10 min at 4°C. The supernatant was passed through a nylon mesh (pore size 20µ) and about 1.5 volumes of stabilization buffer (Table 5) was added to 1 volume of filtered supernatant SN1. The pellet P1 was resuspended with the homogenization buffer and the same process was repeated to get the SN1 again. About 1.5 volumes of stabilization buffer (Table 2.5) was added to 1 volume of filtered supernatant SN1. Both SN1 were combined and continued with differential centrifugation.

Differential centrifugation

The supernatant SN1 (nylon mesh filtered and combined) was centrifuged at 3000 × g for 10 min at 4°C. The supernatant (SN2) was carefully removed (Avoid transferring any pelleted material (P2)). Again, the supernatant SN2 was centrifuged at 10,000 × g for 15 min at 4°C. The obtained supernatant (SN3) was carefully removed and the pelleted mitochondria (P3) was resuspended with maintenance buffer (10 mM Tricine, 5 mM NaCl, 210 mM mannitol, 70 mM sucrose, pH adjusted to 7.4 with Bis-Tris).

In addition to the SHSY5Y cell samples, the chicken liver cells (about 700 mg) were also homogenized using normal dounce homogenizer followed by differential centrifugation. The cell pellets and the supernatants obtained at different centrifugal speeds were proceeded for the blue native gel electrophoresis.

B. Mitochondrial isolation kit (Dounced homogenization)

Part 1:

The cells were grown in 75 cm^2 flask. After the cells were 80-90% confluent, the cells were washed with prewarmed DPBS (sterile) once. The cells were then digested with 0.25% trypsin and DPBS solution for 3 min in a humidified cell incubator with 37°C and 5% CO_2 so that the majority of the cells get detached. The reaction was stopped by adding 5 ml cold DMEM with 10% FBS and was centrifuged at 900 rpm (100 x g) for 5 min at 4°C. The supernatant was discarded and the pellet was washed with cold PBS and centrifuged again. During centrifugation, immediately before use, Protease inhibitor was added to reagent A and reagent C (inhibitor was added to the reagent, only in that amount being used for the procedure and not to the stock solutions). Dounce homogenizer was pre-chilled on ice before use. 800 µl of mitochondrial isolation reagent A was then added to the obtained pellet and vortexed at medium speed for 5 sec. The tube was cautiously incubated on ice for exactly 2 min.

Part 2.

Now, the cell suspension was transferred to Dounce tissue grinder. The cells were homogenized on ice like in method A but the number of strokes was 60. The lysed cells were returned to original tube and 800 µl of Reagent C was added. The Dounce grinder was rinsed with 200 µl of Reagent A and it was added to tube containing the sample with reagent C. The tube was inverted several times to mix (No vortex). The tube was centrifuged at 700 × g for 10 min at 4

°C. The supernatant was transferred to a new tube and again centrifuged at 3000 × g for 15 min at 4°C. Again, the supernatant was transferred to other new tube and centrifuged at 12,000 × g for 15 min at 4°C. The obtained pellet is supposed to be the mitochondrial pellet. 500 µl Reagent C was added to the mitochondrial pellet and centrifuged at 12,000 × g for 5 min at 4° C. The supernatant was discarded and the mitochondrial pellet was maintained in maintenance buffer (Table 2.5) and stored° at -80 °C.

2.2.2.3Percolls gradient method

Percolls gradient method was used after the differential centrifugation of organelle fractionates (Kristian et al, 2006).

The obtained mitochondrial pellet was resuspended in 1.4 ml of homogenization buffer.1 ml of 50% percoll solution as cushion and layer 3 ml of 22% percoll solution were prepared in two 5 ml centrifugal tubes. 0.3 ml of 50% percoll was added to the resuspended pellet (final sample now has the concentration of percoll of 15%) and layer 1 ml of 15% percoll sample on top of the described 50%-22% gradient. 15% percoll was used to help balance the centrifuge tubes and centrifuged at 30700g for 6 min. The mitochondria were recovered from 50%-22% percoll interface.

2.2.3 Proteomics method

2.2.3.1 BCA protein assay

Protein concentration of the samples was determined using Pierce BCA Protein assay kit. The BCA assay is based on bicinchoninic acid (BCA) for colorimetric detection of total protein in the solution (P. Smith, Krohn, Hermanson, & Mallia, 1985). This assay method holds the principle that at first, Cu^{++} is reduced to Cu^{+} by protein in alkaline surroundings and then the colorimetric detection of Cu^{+} cation using a reagent containing BCA. The reaction forms a purple colored product that absorbs light at the wavelength of 562 nm.Absorbance of water soluble BCA copper complex is measured at 562 nm using a 96 well microtiter plate reader. Protein concentration range can be measured over a working range from 20 µg/ml to 2000 µg/ml. All protein concentrations were determined with the reference to a standard curve of known protein standards of bovine serum albumin (BSA). The standard curve was plotted with the absorbance value as the dependent variable (y-axis) and concentration as the independent variable (x-axis) resulted in an equation: $y = ax + b$. Solving for x, by inserting the sample's absorbance value, determined the protein concentration of the sample.

In short, the protein samples of interest were diluted in water to a total volume of 25µl and measured in triplicates. 200µl of the colorimetric reagent were applied to the sample followed by incubation at 37°C for 30 min. The absorbance at 562 nm was measured using a 96 well Micro plater reader. Absorbance measured at 562 nm were then finally translated to protein concentrations using the slope of the standard curve.

2.2.3.2 Blue Native Polyacrylamide Gel Electrophoresis (BN PAGE)

Bis-Tris based precast gel (Invitrogen Native PAGE Gradient gel (3 %- 12 %), 1mm × 10 wells) was used for the separation of the protein complexes of the cells.

Sample preparation for BN PAGE:

The cell pellets and the supernatants obtained after the differential centrifugation were proceeded for gel electrophoresis. All the procedures were carried out on ice. The cell (about 4.2×10^6) were resuspended in maintenance buffer and 10x TMK buffer (Table 2.7). It was then solubilized with digitonin 10% (w/v) digitonin making the final volume of 20 µl. It was incubated on ice for 10 min and snipped lightly followed by the centrifugation for about an hour at 30,000g. Then, 1 µl glycerol was added to the supernatant and was loaded on the BN gel along with the unstained protein marker (3 µl). (Generally, 10-15 µg of protein was loaded on each lane).

Gel electrophoresis condition for BN PAGE:

Firstly, taking the precast Bis Tris gel, the electrophoretic apparatus was assembled. The cathode buffer supplemented with 80 µM LDS and anode buffer (Table 2.6) were used to run BN PAGE gel. The inner chamber was filled with the cathode buffer and the outer chamber was filled with the anode buffer. The gel run was left for overnight under the cold condition at constant 10 mA with limited voltage of 15 V after loading the samples in all gel lanes. The voltage was increased to 150 V with less ampere current on the next morning for the complete gel run.

2.2.3.3 Sodium Dodecyl Sulfate Polyacrylamide Gel Electrophoresis (SDS PAGE)

SDS PAGE gel electrophoresis was carried out in 12.5% SDS PAGE gel to separate out the denatured proteins.

Sample preparation for SDS PAGE

The cell pellets and the supernatants obtained after the differential centrifugation were proceeded for gel electrophoresis. All the procedures were carried out on ice. The cell (about 3 × 10^6 cells) was resuspended in maintenance buffer and 2x sample loading buffer (Table 2.9). It was then centrifuged for about 1 min at RT followed by heating at 85°C for about 2 min. The cell samples were centrifuged for about 15 min at maximum speed at RT and the supernatant was loaded on the SDS gel along with the prestained protein marker. (Generally, 10-15 µg of protein was loaded on each lane).

Electrophoretic conditions for SDS PAGE

SDS gels consisting of 12.5% separating gel and 4% stacking gel were cast as described (Reisinger & Eichacker, 2006). The clean 10 well comb was inserted in between the plates sandwich before stacking gel was poured. After the gel was polymerized, the electrophoretic apparatus was assembled. The cathode buffer supplemented with 0.1% SDS and 2 mM Sodium bisulfite along with the anode buffer as mentioned in Table 2.8 were used to run SDS PAGE gel. The inner chamber was filled with the cathode buffer and the outer chamber was filled with the anode buffer. Each well of the gel was washed (by pipetting up and down) 8-10 times with anode buffer using a micro-syringe before loading the samples onto the gel. The gel run was left for half an hour at RT at constant 150 V after loading the samples onto the gel.

Coomassie staining

The separated protein complexes on gel, after electrophoresis, were visualized using coomassie staining method. The gel was washed initially with distilled water and placed on the shaker for about 15 min. Then the water was replaced with the coomassie staining solution (appendix C). The gel in staining solution was incubated for at least 3 hours (hrs.) (up to overnight) with constant shaking. The distilled water was used to destain the gel for at least 3 times so that the background of gel was clear enough. When background blue colour was not removed well using water, then the water with 20% methanol was used.

The coomassie stained gel was scanned with the help of odyssey scanner and white light scanner.

2.2.3.4 Western blot analysis subsequent to BN or SDS PAGE

The separated Proteins in BN and SDS gel were transferred to polyvinylidene fluoride (PVDF) membranes (GE Healthcare). Firstly, after the gel run, the gel was washed with distilled water two times and then incubated in transfer buffer (Table 2.11) for about 10 min to equilibrate the

gel before the subsequent transfer to the PVDF membrane. Meanwhile, the gel size blotting paper was soaked in transfer buffer. The PVDF membrane was soaked firstly in methanol solution and then in the transfer buffer for some time in shaker. Transfer was performed at 15 V for 30 min. at RT. Assembly of western blot is shown in Figure 2.2.

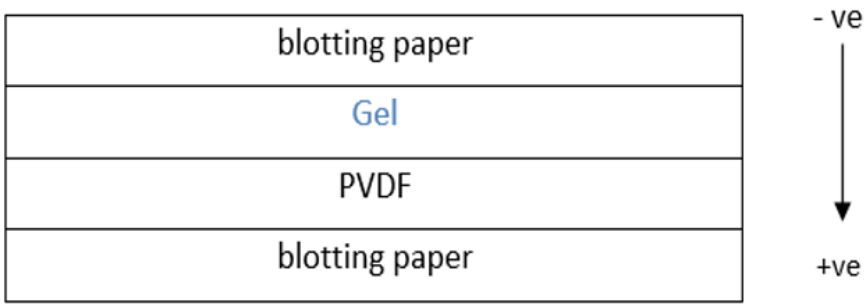

Figure 2.2: Assembly of western blot

After the protein transfer from gel to PVDF, the PVDF membrane was first blocked for some hours with blocking buffer followed by incubation with the 1x blocking buffers solution containing primary antibodies (Table 2.3) in the ratio of 1:1250 (4.5 ml water+500µl Roti buffer+4 µl monoclonal primary antibodies) under cold condition for overnight. The PVDF membrane was washed with the PBS Tween 20 solution (0. 05%). Following three washes in PBS-T for 5 min, secondary antibodies (Table 2.3) were applied at 1:50000 dilution in 1x blocking buffer for 1 hr at RT. Membranes were washed again with the PBS-T (3 × 5 min). Equal volume of ECL reagent 1 and 2 (Table 2.2) were mixed to prepare the enhanced chemiluminescent substrate for the detection of HRP activity from secondary antibodies. Then, the membrane was incubated with ECL substrate on parafilm for about 5 min at RT. The PVDF was then placed in clear plastic pocket and exposed for 15 seconds using a BioRad Chemi Doc Touch instrument to visualize the protein bands.

2.2.4 Drug treatment for the cell SHSY5Y

2.2.4.1 Cell treatment with 6-OHDA

The cells grown in a cell culture flask (75 cm^2) were splitted by trypsination after the cells were about 80-90% confluent. The cells were sub cultured in 24 well plates adjusting the cell density to 50,000 cells per glass slide. Meanwhile, the cells were also sub cultured in two different media, DMEM and NBA in two 96 well microtiter plates (VWR Tissue culture plate), adjusting the cell density to 20,000 cells per glass slide. All the plates were incubated in a humidified cell

incubator at 37°C and 5% CO_2 until the next day. On the next day of initial seeding, the cells grown uniformly were subsequently exposed to the different concentrations of 6-OHDA. But, immediately before 6-OHDA addition to 24 well and 96 well plates, stock of 6-OHDA (10 mM) was made in DMEM to achieve the required final concentrations. The cells of 24 well plate were exposed to varying 6-OHDA concentrations (0 µM, 10 µM, 25 µM, 50 µM,100 µM and 250 µM) while the cells of 96 well plates were exposed to 0 µM, 2.5 µM, 5 µM, 10 µM, 25 µM, 50 µM,100 µM ,250 µM and 500 µM of 6-OHDA concentrations. The untreated cells served as a negative control. The cells were then incubated in a humidified cell incubator at 37°C and 5% CO_2 until the next day.

The following day, the cells in 24 well plates were washed with the PBS, after aspirating the culture medium and then subsequently fixed with prewarmed 4% paraformaldehyde. The cells were incubated at RT for about half an hour before storing at 4 °C.

To both the cell plates (96 well plates), mixture of XTT and activation reagent (Table 2.1) were added and incubated in a humidified in cell incubator at 37°C and 5% CO_2 for about 5 to 6 hrs. The absorbance reading was done at 450-630 nm for cells treated with 6-OHDA.

The experiment was triplicated to ensure the result.

2.2.4.2 Cell staining

The 6-OHDA treated cells fixed with paraformaldehyde was proceeded for staining. The parafilm was attached on the tip boxes, with the water soaked towel paper inside the box. The slips were placed on the parafilm and washed once with the PBS at RT. It was then incubated with 0.5% Triton X100 in PBS for about 15 min in order to permeabilize the cells. The cells were then subsequently washed with PBS (2 × 5 min). It was incubated with the blocking solution (20% FCS/PBS-TWEEN 0.2%) for an hour at RT. The blocking solution was aspirated and again incubated at 4°C overnight with the diluted primary antibodies (Table 2.4) in blocking solution (centrifuged at 10000 rpm for 2-5 min). The following day the antibody was removed and the cell slides were washed with PBS (4×5 min). Subsequently, the cells were incubated with secondary antibodies (Table 2.4) in blocking solution (centrifuged at 10000 rpm for 2-5 min) for 1 hr at RT under dark condition. The cells were then stained with Hoechst 33342 diluted 1:1000 (2 µg/ml) in PBS for about 2 min after removing the secondary antibodies. The Hoechst 33342 was collected separately followed by the subsequent PBS wash (4×5 min). The cell slides were mounted in Mowiol 4-88 (appendix-D) and was let it dry in dark overnight at RT.

2.2.4.3 Immunofluorescence microscopy

Samples were examined using Nikon immunofluorescence microscope Nikon A1R, equipped with the appropriate filter combination and a 60x objective lens. Fluorescence images were acquired with a Nikon Software. Digital images were optimized for contrast and brightness using imagej.

3 RESULTS

3.1 Determination of protein concentration

The cell samples were homogenized and centrifuged subsequently followed by BCA assay. All the protein concentrations determined for the protein sample of interest, using BCA protein assay as mentioned in methods, were found to be in the range from 2-483 µg/ml (appendix A).

3.2 Isolation of intact mitochondria and its analysis by BN, SDS PAGE and Western blot

As the mitochondria is believed to have the immense role and its dysfunction is responsible for the different neurodegenerative disease like PD, the study of mitochondrial protein has been the matter of paramount concern. The isolation of the pure intact mitochondria to study its role in various neurodegenerative disease is quite a matter of essence. To isolate the intact mitochondria from the neuroblastoma cell line SHSY5Y, the whole cell sample was initially homogenized and the cell fractionates (pellets and the supernatants) of each differential centrifugation steps were analyzed by BN PAGE, SDS PAGE and the subsequent western blot analysis. The western blot analysis was carried out probing the membrane PVDF with monoclonal rabbit anti COXIV antibody (Table 2).

A workflow of the methods used in this study are shown in Figure 3.1.

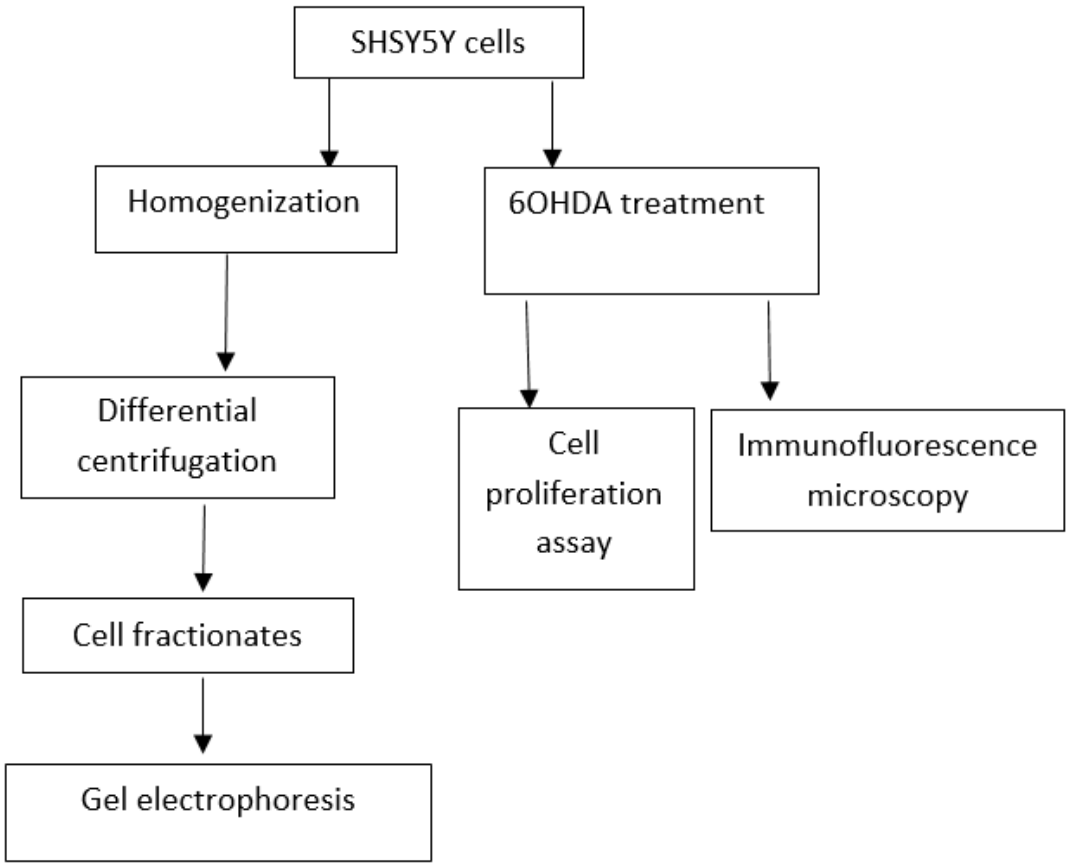

Figure 3.1: Method workflow. The SHSY5Y cells were subjected to the intact mitochondrial isolation and the effect of 6-OHDA was analyzed using the various methods as shown in flow diagram.

Initial experiments using cells grown on 75 cm^2 culture flask revealed that the cell count had to be increased due to very low yield. So, during the entire process, the cells were harvested from the big cell culture flasks (175 cm^2) using the trypsination method that could produce the enough cell fractionates and the proteins for the proteomics study.

The harvested cells were first subjected for the mitochondrial isolation using both normal dounce homogenization (DH) and dounce homogenization mentioned in mitochondrial isolation kit (DH: MIK) as mentioned in section B of methods. The protein complexes were separated from the cell fractionates obtained from the differential centrifugation on BN PAGE (7.5%). Figure 3.2A shows a coomassie stained BN PAGE gel of cell fractionates.

To prove that the mitochondrial fraction (P3) actually contain mitochondria, western blots stained for the mitochondria-specific protein Cox IV (Figure 3.2B).

A. B. .

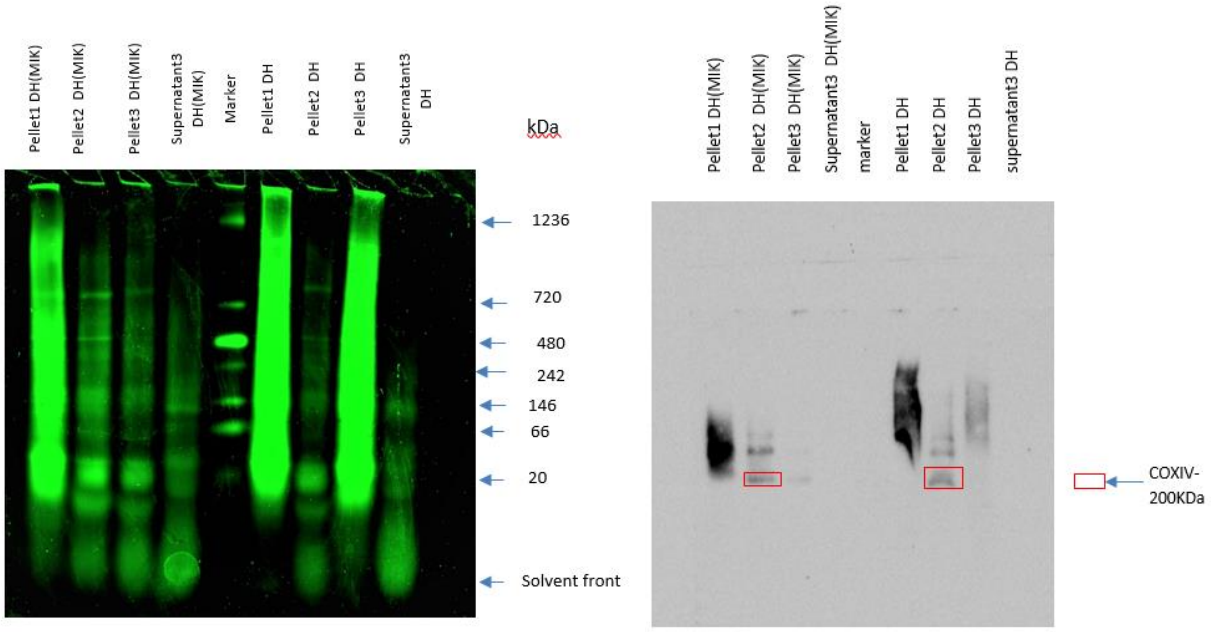

Figure 3.2: Comparision of normal Dounce homogenization method (DH) and Dounce homogenization of mitochondrial isolation kit (DH: MIK). Protein complexes, obtained using normal Dounce homogenization method (DH) and Dounce homogenization of mitochondrial isolation kit (DH: MIK) separated from the cell fractionates by BN PAGE on 7.5% Bis Tris gel **A.** Odyssey scanned gel image **B.** Western blot image probed with anti COXIV antibody**.** The protein complexes from the cell fractionates obtained from the differential centrifugation of cell samples as mentioned in methods using both DH and DH(MIK) were separated by BN PAGE followed by subsequent coomassie staining and scanning in Odyssey scanner. For the BN gel run simultaneously with the next similar cell samples under similar condition, the western blot was carried out after the protein complexes were transferred to PVDF membrane from BN gel.

The coomassie stain for the separated membrane protein complexes was observed (Figure 3.2A). The mitochondrial protein complex COXIV (200 KDa) was detected on pellet 2, obtained for both the DH (normal dounce homogenization) and DH(MIK) methods (Figure 3.2B). DH method has some indication that there is mitochondrial protein in pellet 3 (less in DH: MIK). However, both methods seem to lose mitochondrial fractions prior to pellet 3. Thus, these results suggested that the use of DH could be relatively the promising method for the pure mitochondrial isolation.

Intrigued, the normal dounce homogenization method (other than mentioned in mitochondrial isolation kit) was followed now onward. The proteins and the protein complexes from the cell fractionates of differential centrifugation were subsequently separated on SDS PAGE and BN PAGE respectively. The SDS gel was stained with the coomassie blue and scanned with the odyssey scanner (Figure 3.3A) and BN PAGE gel was stained with the coomassie blue (Figure 3.3B).

A. B.

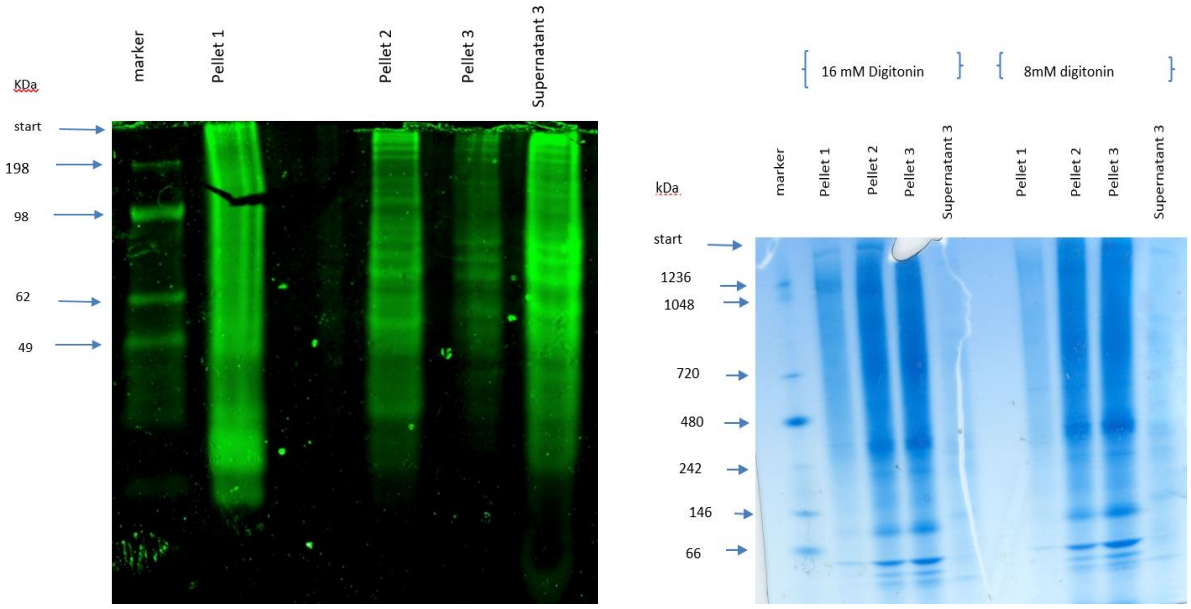

Figure 3.3: Resolution of the protein and protein complexes using SDS and BN PAGE respectively. A) Oddysey scanned SDS gel image **B)** Coomassie blue stained BN gel image. In both figures, pellet 1 was obtained at 800 × g for 10 min, pellet 2 was obtained at 3000 × g for 10 min and pellet 3 was obtained at the 16000 × g for 30 min. Supernatant 3 was of 16000 × g for 30 min. The separated proteins and the protein complexes from pellet 3 were found to be observed in pellet 2 as well. In Figure B, the left side and the right side depict the use of two different concentrations of digitonin for solubilizing the membrane protein complexes.

The proteins separated in SDS PAGE gel (Figure 3.3A) looked similar in the lanes of pellet 2, 3 and supernatant 3. Likewise, the protein complexes separated on BN PAGE gel (Figure 3.3B) also looked similar in composition in pellet 2 and pellet 3 lanes. These indicate that there was no or

little fractionation (all fractions have the same composition) which could be due to too harsh homogenization processes and was thus, beyond the expectation. The membrane protein complexes were separated, on 7.5% Bis Tris gel, in equal and comparable distribution by using 8 mM and 16 mM digitonin (Figure 3.3B).

As the mitochondria isolated from the SHSY5Y cells proved difficult, the fresh chicken liver cells (700 mg) were homogenized using normal dounce homogenization (DH) and performed differential centrifugation at the same speeds to isolate the mitochondria. The protein complexes from the cell fractionates obtained were separated by BN PAGE on 7.5% Bis tris gel and was stained on coomassie blue (Figure 3.4).

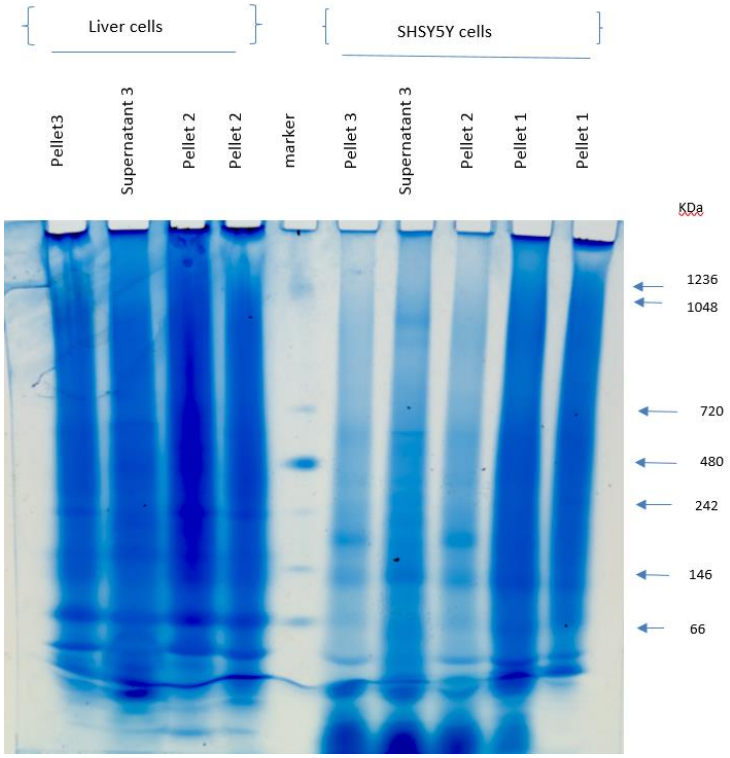

Figure 3.4: Resolution of the protein complexes from the cell fractionates by BN PAGE on 7.5% Bis tris gel. The left side and the right side of a unstained protein marker show the separated protein complexes for the chicken liver cells and SHSY5Y cells respectively.

The protein complexes separated in case of both liver cells and the SHSY5Y cells by BN PAGE (Figure 3.4) were similar in the pellet 2 and 3 lanes. The presence of mitochondrial membrane protein complex in both pellet 2 and 3 indicated that the pure mitochondria was still not obtained.

So, now, the plan was to adjust the centrifugation steps to increase the yield of mitochondria in pellet3. Following the same experimental methods but decreasing the centrifugal speeds, the cell fractionates were made to run on SDS gel and the separated proteins from SDS gel were subsequently transferred to PVDF membrane for western blot analysis (Figure 3.5).

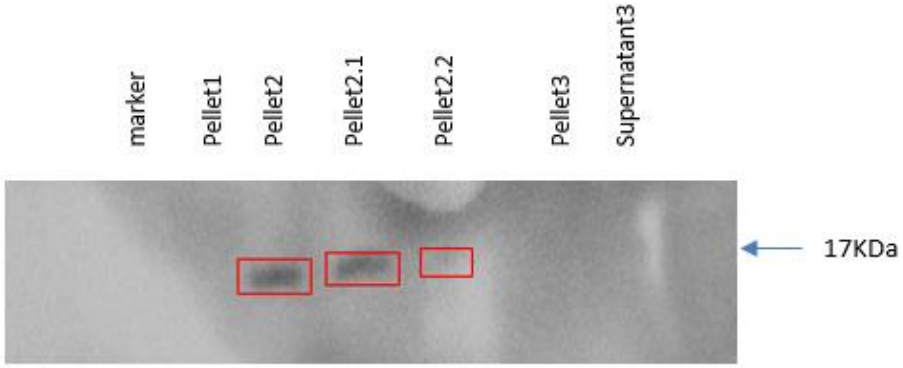

Figure 3.5: Western blot image probed with anti COXIV antibody. The red boundary box denotes the detected COXIV protein (16 KDa) of mitochondrial membrane, observed in the lanes of pellet 2, 2.1 and 2.2. The pellet 1, 2, 2.1 and 2.2 were obtained at the differential centrifugation of 800 × g, 1600 × g, 2800 × g and 3500 × g for 10 min. The pellet 3 and supernatant 3 were obtained at 16000 × g for 30 min. The protein separated by the SDS-PAGE was subsequently transferred to PVDF.

It was observed that the mitochondrial protein COXIV (16 KDa) was present in all pellets; pellet 2, 2.1 and 2.2. It indicates that the mitochondria were pelleted down even at the lower centrifugal speeds with the other cell components smaller than the nuclei and the unbroken cells. So again, the centrifugal speed was lowered further for the pellet 2 fractions assuming the cell components smaller than the nuclei could be pelleted down with no mitochondrial contamination. The BN PAGE and SDS PAGE were run for the cell fractionates obtained by optimization.

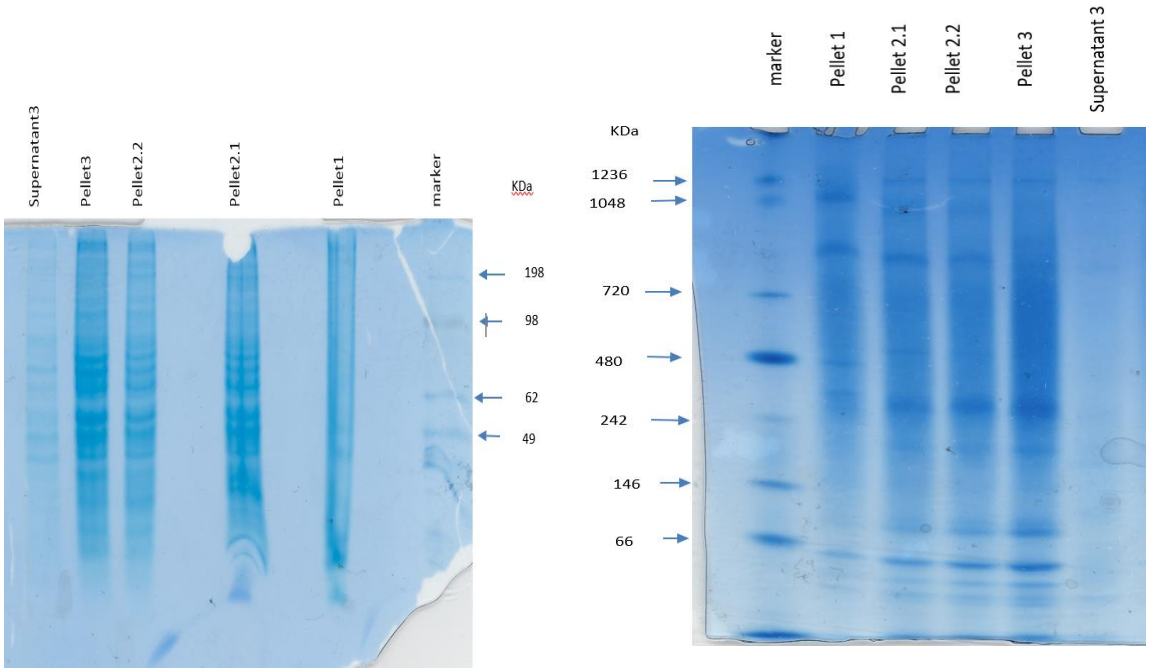

Figure 3.6: Separation of the proteins and protein complexes from the cell fractionates by gel electrophoresis. (A) SDS PAGE **(B)** BN PAGE**.** Pellets 1, 2.1, and 2.2 were obtained at 800 × g, 1600 × g and 2400 × g for 20 min respectively. Both Pellet 3 and supernatant 3 were obtained at 16000 × g for 30 min.

Surprisingly, the proteins separated on SDS gel had again almost the similar composition in all lanes of pellet 2.1, 2.2 and 3, regardless the lower centrifugal speeds (Figure 3.6A). The membrane protein complexes separated by BN PAGE on 7.5% Bis Tris gel had also similar composition on the lanes of pellet 2.1, 2.2 and 3 (Figure 3.6B) despite the lower centrifugal speed for pellet 2 fractions. So, finally the results reflected that the pure intact mitochondria were not obtained with the dounce homogenization method followed by the subsequent differential centrifugation.

3.3 Effect of 6-OHDA on neuronal cells SHSY5Y

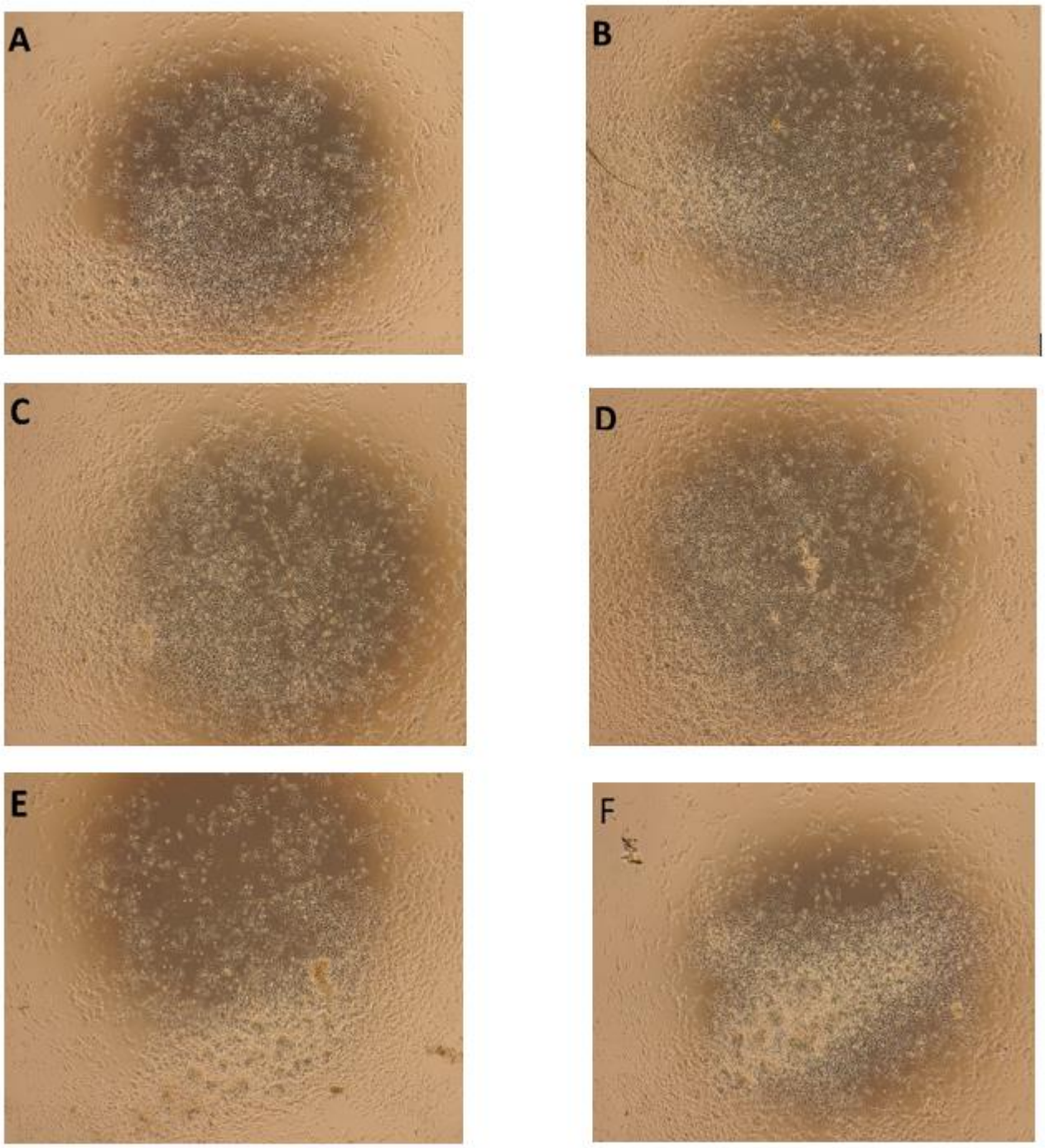

Figure 3.7: The normal cell numbers and cell shapes of SHSY5Y cells before exposure to 6-OHDA. The SHSY5Y cells, after 24 hrs of initial seeding, were found to be grown uniformly in each well. The cells were sub cultured adjusting the cell density to 50,000 cell/well incubating in a humidified incubator**.**

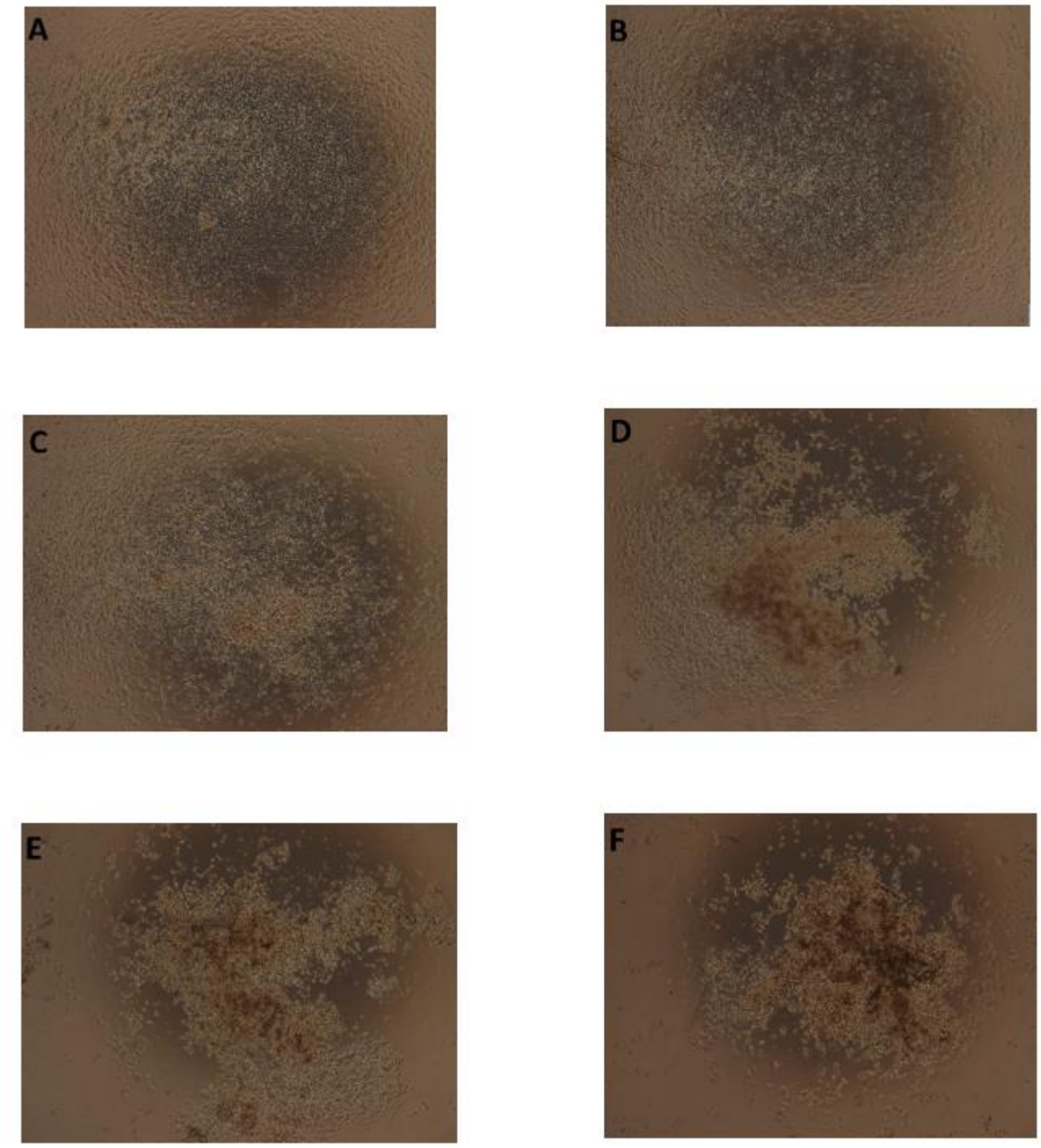

Figure 3.8: The cell numbers and cell shape after exposure to various 6OHDA concentration. The effect of different concentrations of 6-OHDA after 24 hrs incubation on the cell shape and cell number of SHSY5Y cell were observed. A. 0 µM (control) B.10 µM of 6-OHDA C.25 µM of 6-OHDA D.50 µM of 6-OHDA E.100 µM of 6-OHDA F.250 µM of 6-OHDA.

The SHSY5Y cells, morphologically neuroblast like non-polarized cell bodies with few truncated process, tend to grow in clusters and formed clumps as cells appear to grow on top of one another in central region of cell mass (Figure 3.7).

But, the cells exposed to varying concentrations of 6-OHDA, after 24 hrs. incubation, resulted in distorted shaped cells and cell death (Figure 3.8). It specified the profound effect of neurotoxin 6-OHDA on neuroblastoma cells (SHSY5Y) at different concentrations.

3.3.1 Dose response relationship of 6-OHDA cytotoxicity

6-OHDA, as a cytotoxic agent, caused a significant dose related decrease of cell viability, measured using XTT reagent method in SHSY5Y cells (Figure 3.9). The incubation of the 6-OHDA treated cells with the XTT reagent for about 6 hrs produce the orange color dye whose intensity is directly proportional to the number of metabolically active cells. The dye formation decreased with the higher concentration of 6-OHDA indicating the reduction in survival of cells. The IC_{50} value from the toxicity curve was found to be about 63 µM (Figure 3.9).

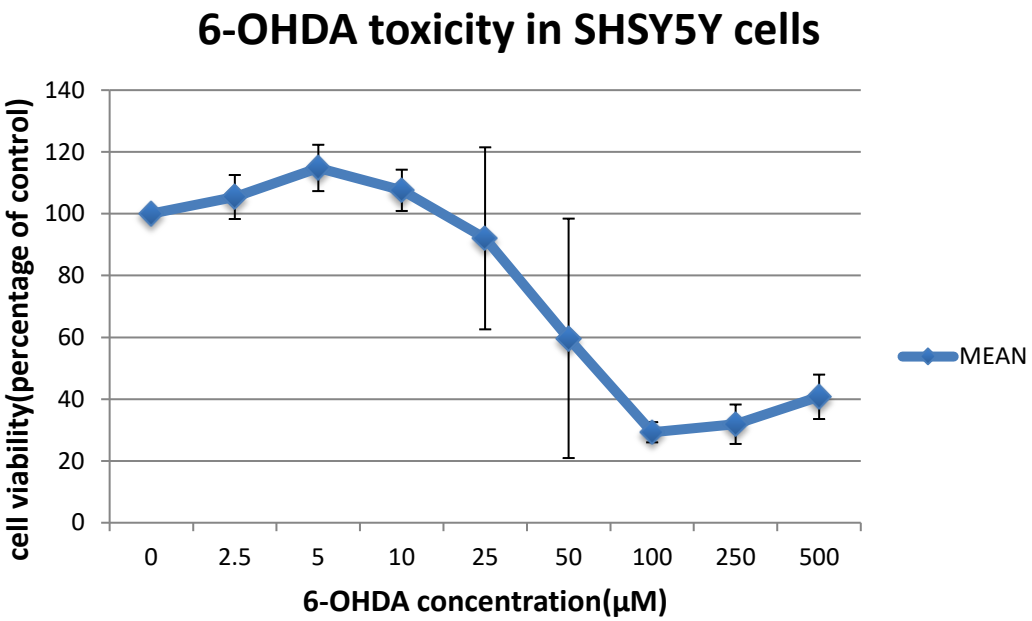

Figure 3.9: Effects of 6-OHDA on the viability of SHSY5Y cells. The cells exposed to different concentrations of 6-OHDA in 96 well plate for 24 hrs. were assayed using XTT reagent method and represented as the percentage of untreated control (in the absence of 6-OHDA). Each point represents the mean ±SEM (n = 4). The 6-OHDA treated cells were incubated with XTT and activation reagent in a humidified cell incubator for about 6 hrs. The absorbance reading in the spectrophotometer produced the dose response relationship curve as shown above. The survival rate of the cells is increasing slightly at the lower concentrations of 6-OHDA but above 10 µM concentration, there is significant decrease in cell survival rate upto the 6-OHDA concentration of 100 µM.

3.3.2 Effects of 6-OHDA on different cell proteins

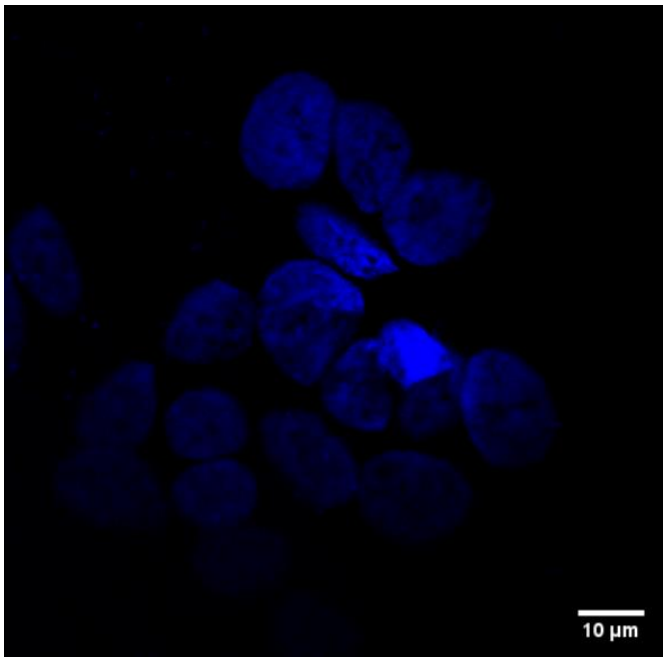

Figure 3.10: Representative Immunofluorescence image of SHSY5Y cells(zoom-2x) (negative control), obtained for the experiments with triplicate. The SHSY5Y cells were fixed with 4% paraformaldehyde followed by the immunofluorescence staining. The nuclei are stained by Hoechst nuclear staining. Scale bar:10 µm

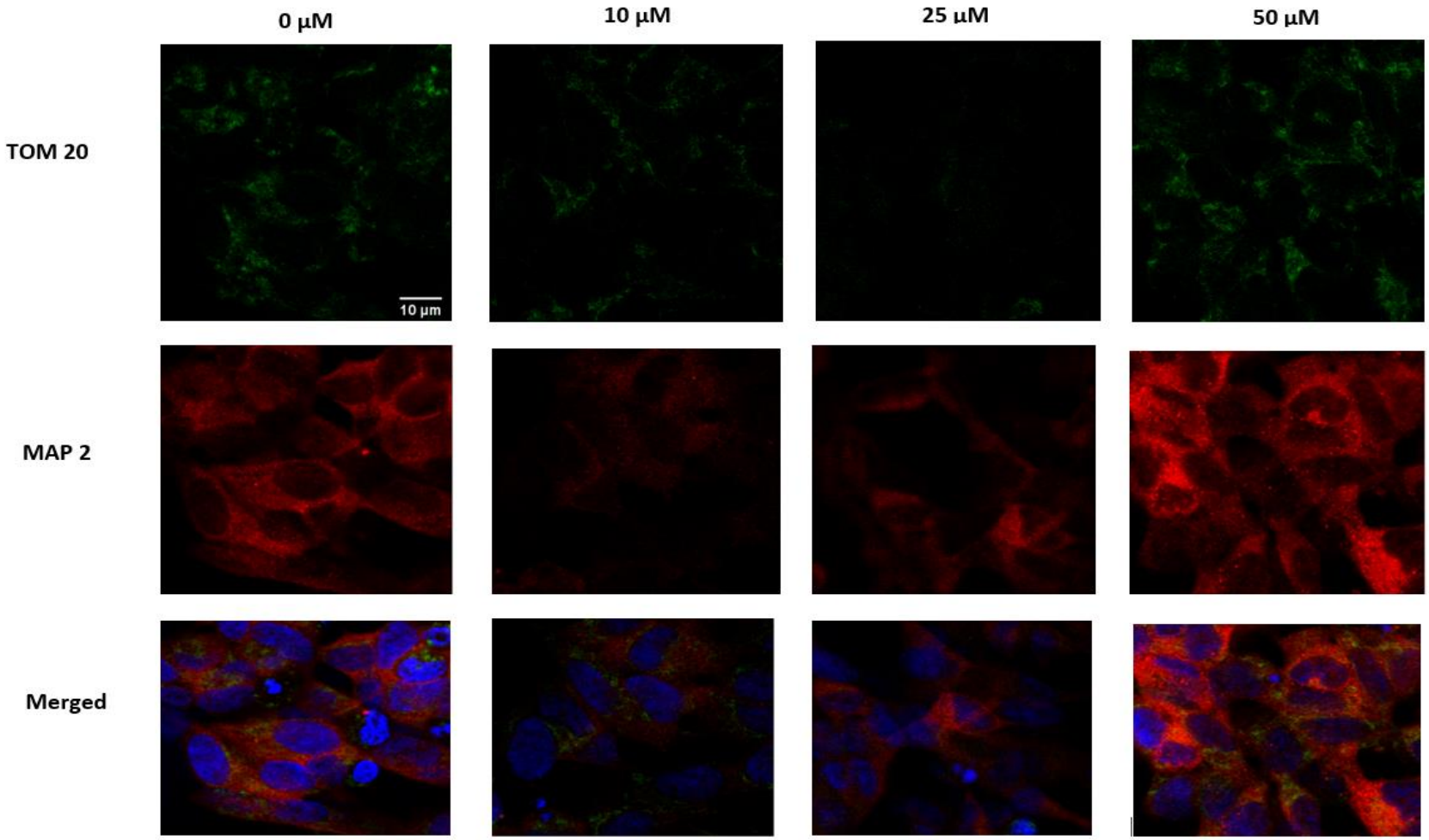

Figure 3.11: Representative Immunofluorescence image of SHSY5Y cells (zoom-3x), obtained for the experiments with triplicate. SHSY5Y cell culture exposed with varying concentrations of 6-OHDA were fixed with 4% paraformaldehyde followed by the immunofluorescence staining. Immunofluorescence imaging shows the localization of fluorescent staining for the mitochondria-specific TOM20 (green) and the microtubule targeted MAP 2 (red). In the merged picture, the nuclei are blue due to the Hoechst nuclear staining. Scale bar :10 µm

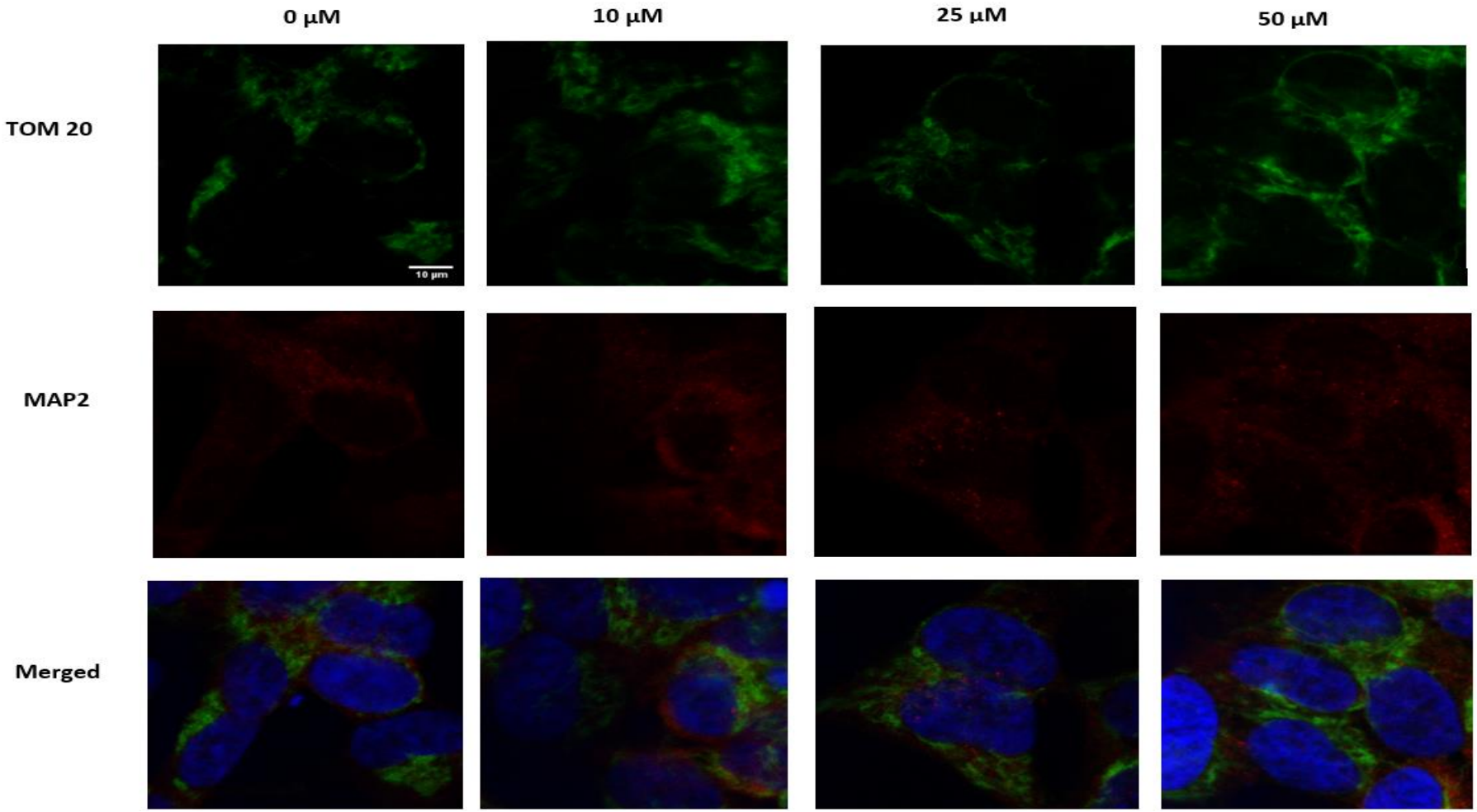

Figure 3.12: Representative Immunofluorescence image of SHSY5Y cells(zoom-5x), obtained for the experiments with triplicate. SHSY5Y cell culture exposed with varying concentrations of 6-OHDA were fixed with 4% paraformaldehyde followed by the immunofluorescence staining. Immunofluorescence imaging shows the localization of fluorescent staining for the mitochondria-specific TOM20 (green) and the mitcrotubule targeted MAP 2 (red). n the merged picture, the nuclei are blue due to the Hoechst nuclear staining Scale bar: 10 µm

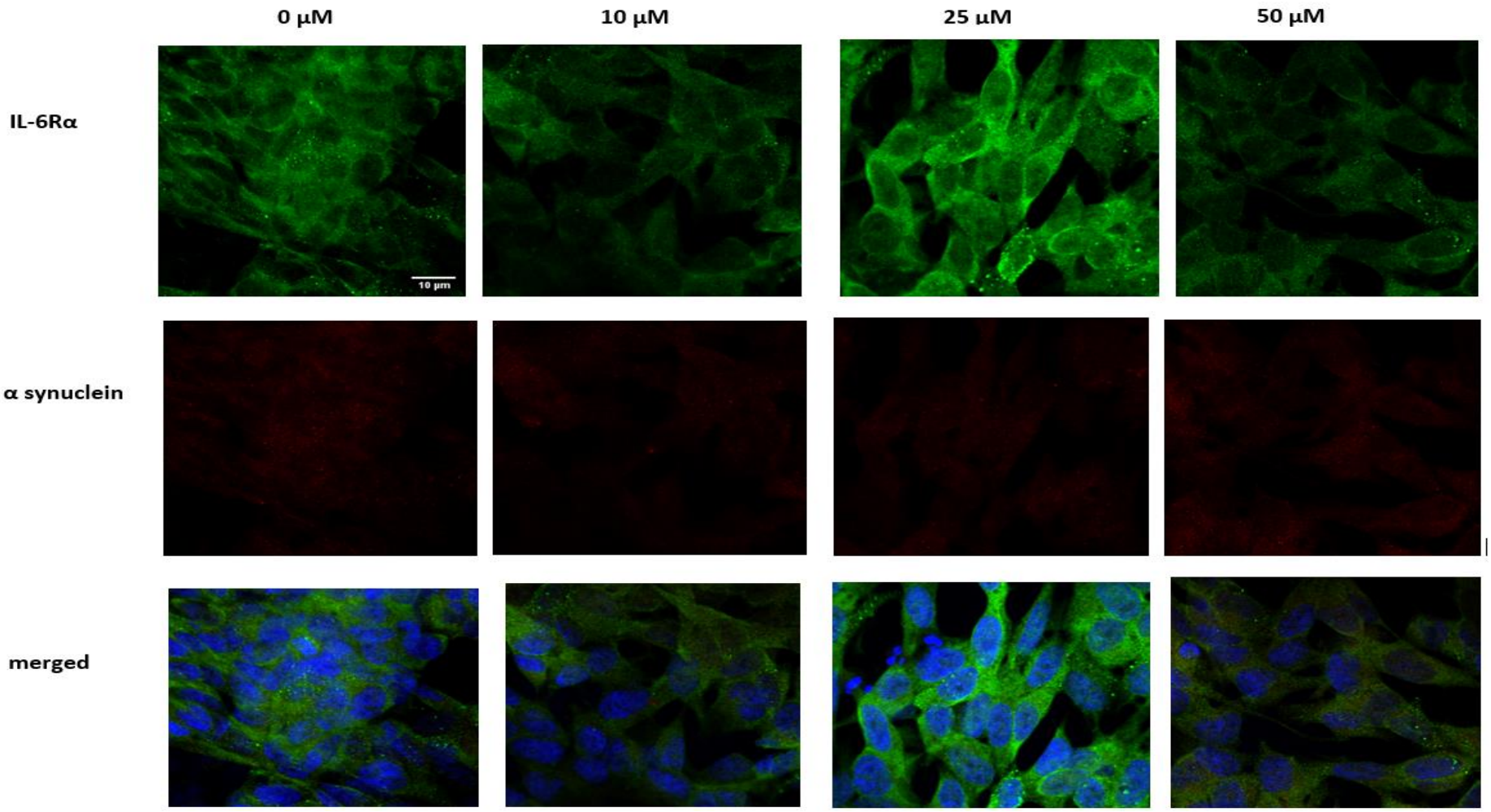

Figure 3.13: Representative Immunofluorescence image of SHSY5Y cells (zoom 2x), obtained for the experiments with triplicate. SHSY5Y cell culture exposed with varying concentrations of 6-OHDA were fixed with 4% paraformaldehyde followed by the immunofluorescence staining. Immunofluorescence imaging shows the localization of fluorescent staining for the alpha-synuclein (red) and the IL-6Rα (green). In the merged picture, the nuclei are blue due to the Hoechst nuclear staining Scale bar: 10 µm

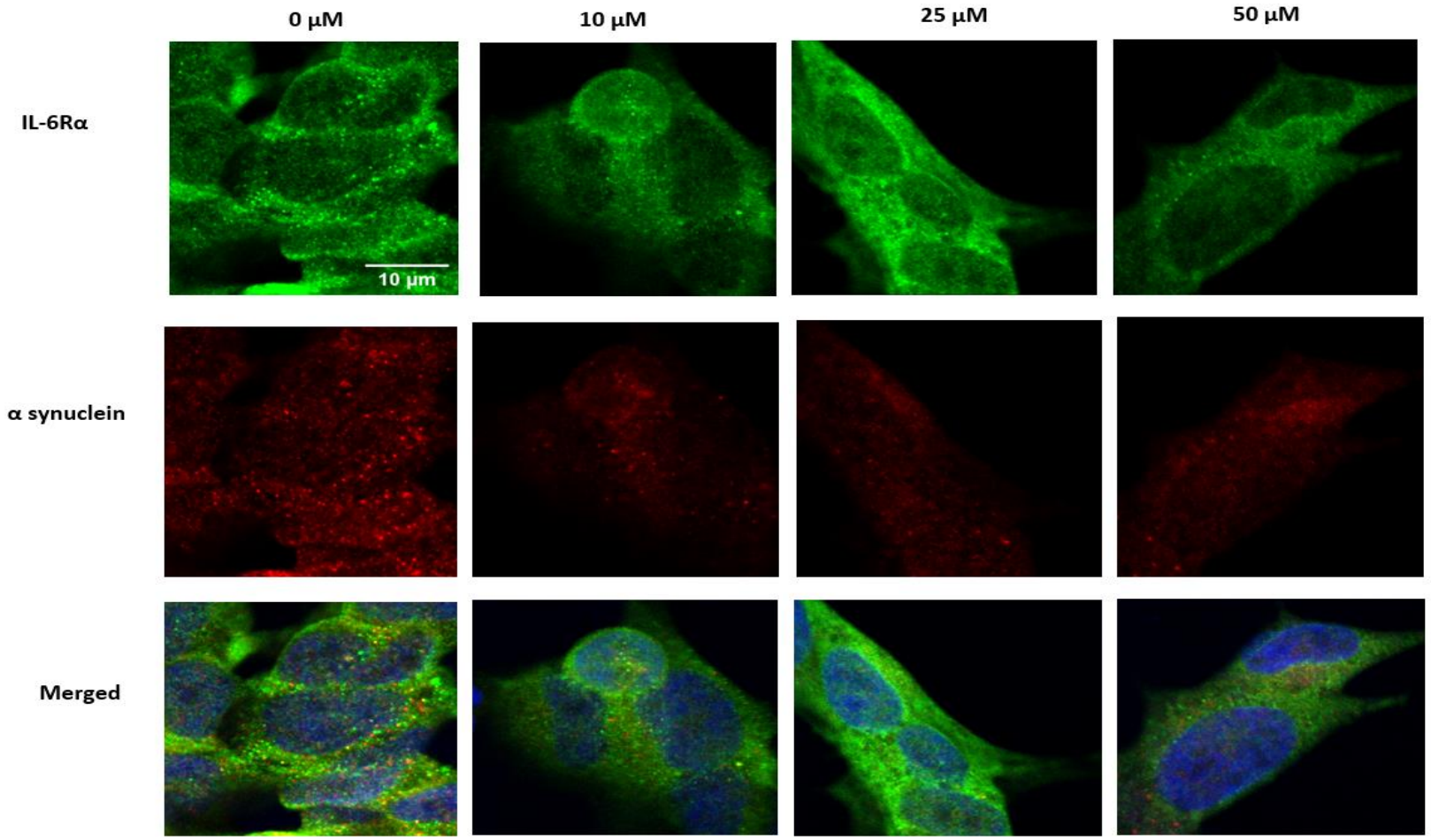

Figure 3.14: Representative Immunofluorescence image of SHSY5Y cells (zoom- 5x), obtained for the experiments with triplicate. SHSY5Y cell culture exposed with varying concentrations of 6-OHDA were fixed with 4% paraformaldehyde followed by the immunofluorescence staining. Immunofluorescence imaging shows the localization of fluorescent staining for the alpha-synuclein (red) and the IL-6Rα (green). In the merged picture, the nuclei are blue due to the Hoechst nuclear staining. Scale bar: 10 µm

6-OHDA was found to have some effect on both TOM20 and cytoskeletal body (MAP2) of neuronal cells SHSY5Y (Figure 3.11 and 3.12). With the increase in 6-OHDA concentration, the expression of both TOM20 and MAP2 in SHSY5Y cells were found to be in decreasing manner except at 6-OHDA concentration of 50 μM.

Also, 6-OHDA was found to have pronounced effect on both protein alpha-synuclein and IL-6Rα in neuronal cell SHSY5Y (Figure 3.13 and 3.14). The expression of alpha-synuclein was found to be slightly decreasing with the increase in 6-OHDA concentration from 10 to 50 μM and the expression of IL-6Rα was found to be decreasing from 0 μM to 50 μM 6-OHDA concentration except at 25 μM.

4. DISCUSSION

The main aim of this study was to isolate the mitochondria in pure intact form for proteomics study and to study the effect of neurotoxin 6-OHDA on SHSY5Y cells. We wanted to analyze the effect of the neurotoxin 6-OHDA on TOM20 in mitochondria, alpha-synuclein, IL-6Rα and the cytoskeletal body of neuron (MAP2) in SHSY5Y cells.

4.1 Mitochondrial isolation

The fact with the importance of mitochondria in the regulation of different cellular processes has broadened their key roles in the neurodegenerative diseases. The growing evidence have addressed the robust association of mitochondrial dysfunction with the neurodegenerative diseases like PD, wherein the impaired mitochondrial function, presumably, leads to the apoptotic cell death (Henchcliffe & Beal, 2008; Lin & Beal, 2006). As such, its isolation from the cultured cells in pure intact form has been an instrumental part of the proteomics study and obviously, a challenging task. Different scientific papers have elucidated various methods for the isolation of mitochondria from the cultured cells and the organs like rat livers as well. However, the homogenization of the cell followed by the differential centrifugation has been the most common and convenient method for the mitochondrial isolation. The slow centrifugation step pellets down the broken cells and cell debris while the subsequent fast centrifugation step sediments the mitochondria (Kappler et al., 2016a).

The release of the cellular constituents with the proper cell membrane disruption is the preliminary step in the isolation of pure intact membrane-bound organelles, which can be achieved using suitable homogenizer. Among the different homogenizer available, the frequently used Dounce homogenizer, firstly used for plasma membrane isolation (Jr, 1960), has gained its popularity in the isolation of subcellular fractionates since then, due to its reliability, cost effectiveness and the convenience (“Chapter 2 Methods of cell breakage: assessing their suitability and efficacy,” 1979).

Based on our study, the results obtained using normal dounce homogenization method indicated that the mitochondria isolated are not pure enough as the mitochondrial proteins resolved by both BN PAGE and SDS PAGE has the similar composition in pellet 2 and 3. The western blot analysis of the membrane proteins separated on BN and SDS gel ensured our results suggesting that the mitochondria isolated were not pure intact. The result resembled with the result obtained for the

mitochondrial isolation for the chicken liver cells under the same procedure (Figure 3.4), depicting the fact of the presence of intact mitochondria in pellet 2 again. Since the intact mitochondria, which was supposed to be only in pellet 3 of higher centrifugal speed (16000 × g for 30 min), got pelleted in pellet 2 along with the other cell components like lysosomes and microsomes except the cell nuclei and unbroken cells (pellet 1), it was confirmed that the mitochondria isolated were still contaminated.

So, taking this problem into account, we speculated that the cell components smaller than the cell nuclei, which were in pellet 2 (centrifugal speed 3000 × g), could be pelleted down at the centrifugal speed lower than 3000 × g. But still, the protein composition in the pellets 2 and the pellet 3 were similar (Figure 3.6) suggesting that the homogenization method we applied, was not appropriate enough in producing the cell fractionates in intact form. The presence of mitochondrial fraction even in less centrifugal speeds as low as 1600 × g clearly indicates the uneven homogenization of cell sample. Despite the fact that many scientific research papers has emphasized on the use of dounce homogenization and the subsequent differential centrifugation method for the mitochondrial isolation from the cultured cells (Clayton & Shadel, n.d., 2014; Kappler et al., 2016b), the mitochondria isolated from SHSY5Y cells during the whole experiment was likely the impure mitochondrial fraction. Many reasons could have undermined the procedure that yielded the impure mitochondria. We can assume that the uneven breakage of cell organelles (number of strokes of pestle A and B) could be due to the use of manually operated homogenizer though it was highly convenient. Possibly, the isolation process could have been very harsh which might have broken the mitochondria subsequently releasing its constituents in SN3. On the next side, the incomplete breakage of cells could have brought down the mitochondria with other unbroken cells during the differential centrifugation. Also, getting the mitochondrial fractions even at lower centrifugal speed than the expected speed suggests that the cells might have been broken incompletely along with the inadequate breakage of the mitochondrial network. Any of these factors or most likely, their combination could be responsible for the results, we obtained. It was difficult to isolate the pure intact mitochondria in a reproducible manner following the published protocols, to carry out the subsequent research and was beyond the expectation.

Though the homogenization was carried out gently avoiding the greater force, the situation could not be improved. Most likely, in addition to the highly variable samples produced by the use of

such manual cell homogenizer that entails the principle of shearing force, the repeatedly produced heat and the shearing stress due to the friction between the cells and the pestle, could have damaged the integrity of cell organelles (Burden, 2008; "Chapter 2 Methods of cell breakage: assessing their suitability and efficacy," 1979; Wettmarshausen & Perocchi, 2017). J. Wettmarshausen et al.2017, lately thus highlighted on the use of nitrogen cavitation for the disruption of the plasma membrane which can yield the intact mitochondria-enriched fractions in a reproducible manner.

The intact mitochondrial isolation process for chicken liver cells as well using dounce homogenization followed by subsequent differential centrifugation didn't give the expected result. It could be due to the ineffective homogenization of solid tissue (grinded liver cells) (Burden, 2008). From our findings, we envisaged that the pure intact mitochondria could not be isolated from the cultured cells with the exclusive use of dounce homogenizer which completely resembles with the hypothesis of Lodish et al., 2000. It is likely that the isolated organelle fractions are not totally pure organelle fractions until and unless the density gradient method is applied for the organelle fractions obtained by differential centrifugation (Lodish et al., 2000; Wieckowski, Giorgi, Lebiedzinska, Duszynski, & Pinton, 2009). So, the percolls gradient method was ultimately applied accordingly after the mitochondrial fraction was obtained with the differential centrifugation of homogenized cells (Kristian et al, 2006). But, the failure of mitochondrial recovery from percoll interface after the centrifugation of 30700 × g for 6 min, accompanied by indistinct mitochondrial layer could have different reasons. The one most probable reason could be the very small mitochondrial pellet (small cell sample) obtained after differential centrifugation (Wieckowski et al., 2009) and the other could be the less centrifugal speed than required (40000 rpm for several hours, impossible in our lab) (Lodish et al., 2000).

4.2 Effect of 6-OHDA on cells

4.2.1 Cytotoxic effect

To date, the oxidative stress associated with the ROS has been considered the fundamental cause for the 6-OHDA induced cellular death though the precise underlying molecular mechanism has not been unraveled (Blum et al., 2001; Iglesias-González et al., 2012; Song et al., 2010). The oxidation products of 6-OHDA, quinone and indole derivatives, as well as the oxyradicals and hydrogen

peroxide have been supposed to have a prominent role in causing the cell death through the cascade of toxic events (Michel & Hefti, 1990). However, the neurotoxicity of this agent has also been linked with the inhibition of respiratory chain enzymes via the involvement of 6-OHDA itself rather than its oxidation product (Glinka & Youdim, 1995) and the strong evidence of apoptotic cell death with calcium overload and significant decreased mitochondrial membrane potential by ROS has added the better insight of 6-OHDA cytotoxic effect on neuroblastoma cells (Song et al., 2010) (Figure 4.1).

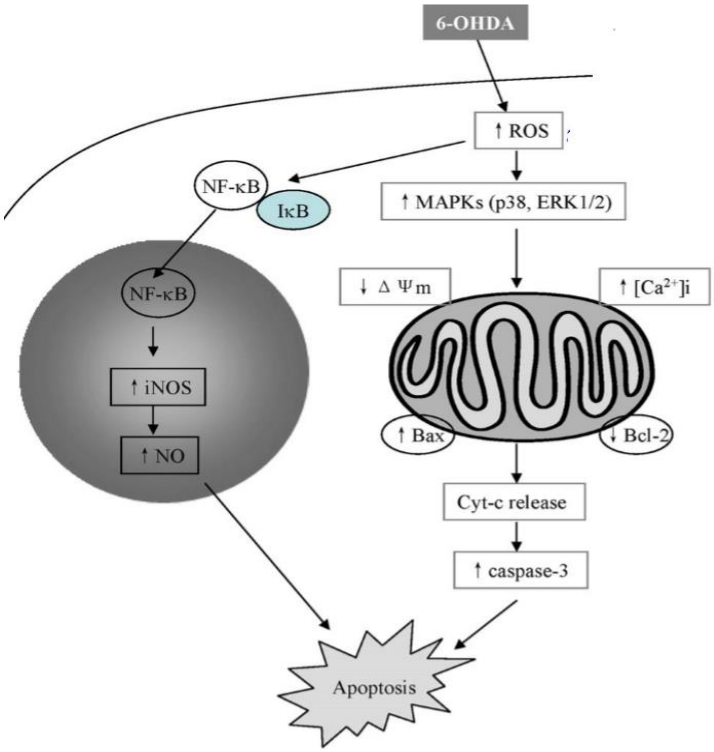

Figure 4.1: Mechanism of 6-OHDA induced apoptotic cell death in neuroblastoma SHSY5Y cells through multiple signaling pathways. ROS generated by 6-OHDA causes: A) MAPKS activation, mitochondrial dysfunction involving decreased mitochondrial membrane potential, increased Ca^{++} influx, imbalance in Bax/Bcl-2 , caspase 3 activation and apoptosis B)Translocation of activated NF-kB followed by increased inducible Nitric Oxide synthase **(**iNOS) and Nitric oxide (NO) leading to apoptosis (Song et al., 2010).

Our findings with the detrimental effects of various concentration of 6-OHDA on SHSY5Y cells regarding the cell viability and the morphological shape (Figure 3.8) sturdily coincides with the

study of L.Wang et al., 2009 (L. Wang, Xu, Xu, & Chan, 2009). The cells were found to be disrupted morphologically when treated with 6-OHDA.

Under our experimental conditions, it has been clear that the cellular death is exquisitely dependent on the concentrations of 6-OHDA. Our results with the 6-OHDA toxicity curve for SHSY5Y cells (Figure 3.9) gives a clear view that the 6-OHDA, with increasing concentration, causes the substantial decrease in cell survival rate. Intriguingly, the IC_{50} value of about 63 µM in our study corresponds closely to the IC_{50} values established in invitro studies of undifferentiated immortalized DA neurons (75 µM :(Clarkson, Edwards-Prasad, Freed, & Prasad, 1999)). Many factors could have interplayed in causing the increasing rate of cell death with the higher 6-OHDA concentrations. As previously stated, various oxidation products of 6-OHDA (Michel & Hefti, 1990),6-OHDA itself inhibiting respiratory chain enzymes (Glinka & Youdim, 1995), significantly increasing ROS level at higher 6-OHDA concentrations resulting high intracellular calcium with decreased mitochondrial membrane potential and subsequent release of Cyt c (apoptosis) (Song et al., 2010) and increased nuclear translocation and binding activity of NF-KB by 6-OHDA(apoptosis) (Levites, Youdim, Maor, & Mandel, 2002; Song et al., 2010) could be the responsible factors for 6-OHDA induced cell death. Interestingly, as explained by Sun et al., 2016 and Kroemer et al., 1998, necrotic cell death likely occurs only at very high 6-OHDA concentrations (above 250 µM, cell incubation of 1 hr. only (Sun et al., 2016)); it can be assumed that the neuronal cell death, in our study, most likely could be due to apoptosis rather than necrosis for the various concentrations of 6-OHDA . As noticed, the deviation is found to be quite high in between the concentration 10 µM and 100 µM, which could be due to the use of varying stock concentrations. So, the actual applied concentration deviates from the intended concentrations. In addition, the cell lines used in different passages and the varying susceptibility of cell lines to 6-OHDA toxicity could be responsible for such discrepant result in our study.

4.2.2 6-OHDA effect on cell proteins

An important aspect of this study is the use of different antibodies to analyze the effects of neurotoxin 6-OHDA on various proteins and morphology of neuronal cell.

The majority of the mitochondrial proteins synthesized in cytosol are transported into the mitochondria with the help of most indispensable protein import machinery, TOM receptors, wherein the TOM 20 involves in recognizing the hydrophobic face of MTS and TOM 22 recognizes the hydrophilic side of MTS presequence at the mean time (Di Maio et al., 2016; Endo & Kohda, 2002). Our study shows that the expression of TOM20 is decreasing with the increase in 6-OHDA concentration (except at 50µM; Figure 3.11 and 3.12). As evinced by many scientific research that the oxidative stress responsible for cell death is generated by 6-OHDA in the neuronal cells, we can believe that 6-OHDA at the higher concentration produces the ROS to the greater extent, causing the ultimate caspase activated apoptotic cell death (Abou-Sleiman, Muqit, & Wood, 2006; Blum et al., 2001; Song et al., 2010). It means that we can believe that along with the decrease in cell survival rate at the higher concentration of 6-OHDA, ROS-related mitochondrial membrane potential collapse could have been increasing simultaneously followed by subsequent apoptosis as evidenced by the lesser expression of TOM20 at the higher 6-OHDA concentration (Lotharius, Dugan, & O'malley, 1999). In addition to this, we can also assume that in order to overcome the stress produced by the higher level of ROS generated at higher 6-OHDA concentration, the mitophagy could have been induced in the neuronal cell as the second line of defense, eventually decreasing the expression of TOM20. Mitophagy induction likely ubiquitinates the larger molecular weight proteins of OMM with the slight ubiquitination of small protein like TOM20 (16 KDa) as well (Rakovic et al., 2013; Zhu et al., 2014). Surprisingly, the higher expression of TOM20 at 50 µM 6-OHDA concentration was noticed which could be due to the inter experimental error. Also, it can be assumed that at higher 6-OHDA concentration, cells could have tried to counteract the effect of 6-OHDA in the other way around to overcome the circumstance which could be responsible for the higher TOM20 expression at 50 µM 6-OHDA. Beside ROS-related toxicity to mitochondria, it can be assumed that the prevalence of less number of mitochondria per cell could be the reason for the lesser expression of TOM20 at the higher concentration of 6-OHDA.

It is well documented that the most abundantly found protein in a neuron, MAP2, comprises the major cytoskeletal body and plays a key role in promoting the microtubule assembly and stability. The normal regulation and the development of neurons with synaptic functions are efficiently controlled by the balanced phosphorylation and dephosphorylation of MAP2, which if gets impaired, can result in neuropathology and neurodegeneration (Sánchez, Díaz-Nido, & Avila, 2000). The striking evidence of 6-OHDA effects on disorganization of microtubule (MT) in

neuronal cells that encompasses the shortening of neurites along with the decrease in MT numbers has strengthened the role of proteins like MAP2 in stable MT assembly (Patel & Chu, 2014). Not surprisingly, the reduced expression of MAP proteins like MAP2 in neuronal cells has been directly correlated with the oxidatively stress- induced destabilization of microtubules (Gardiner, Overall, & Marc, 2013). From our findings of the decreasing expression of MAP2 with the increase in 6-OHDA concentration from 0 to 25 µM, we can assume that the degree of distortion of the MT in the cytoskeleton of SHSY5Y cells could be escalating (Figure 3.11 and 3.12). It might be that the greater ROS level generated by concentrated 6-OHDA can impair the phosphorylation and dephosphorylation of MAP2 which eventually can lead to the neuronal cell death.

Interestingly, ROS can induce caspase activated MAP2 proteolysis followed by subsequent MT depolymerization and ultimate cell death (Ryu & Nakazawa, 2014; Sánchez et al., 2000). This can be the other cause, we can assume, for the lesser expression of MAP2 in SHSY5Y cells exposed to the higher concentration of 6-OHDA. So, the effect of 6-OHDA in the cytoskeletal body of neuronal cell observed likely suggests that the mitochondrial trafficking and all the cellular activities could be perturbed by the oxidative stress, resulting in the ultimate cell death.

It is noteworthy that the neuroinflammation has been highly associated with the microglia mediated inflammation and proinflammatory response in PD, evidenced by the substantial increase in proinflammatory cytokines like IL6 (Hald & Lotharius, 2005; Y.-H. Wang, Xuan, Tian, & Du, 2015). IL6 binds with IL-6Rα, thereby inducing the signal transduction pathway(classical and trans) activating JAK/STAT pathway and MAPK cascades (HEINRICH et al., 2003; J. Smith, Das, Ray, & Banik, 2012; Spooren et al., 2011; S.-W. Wang & Sun, 2014). Though the neurons undergo trans-signaling readily, both types of signaling are possible in neuronal cells that results in the synthesis and secretion of IL6 (Atreya et al., 2000). Mounting evidence reveals that the STAT activation(in particular, STAT3, antiapoptotic), which is directly correlated with the higher expression of IL-6 inducible genes, is found to be disrupted by 6-OHDA in SHSY5Y cells, eventually causing the oxidative stress induced neuronal cell death (Ahmed & Ivashkiv, 2000; Kaur, Lu, Ward, & Halvorsen, 2005; L. Wang et al., 2009). Based on our findings, we can assume that the rate of synthesis of IL6 might be in decreasing manner at the higher 6-OHDA concentration since 6-OHDA disrupts STAT3 pathway as stated earlier. Thus, the less synthesis and secretion of IL6 due to disruption of the STAT3 pathway by 6-OHDA at its higher concentration likely suggests

the likely decrease in binding of available IL6 and IL-6Rα. This could eventually lead to the decrease in expression of IL-6Rα with higher 6-OHDA concentrations. Our findings, in accordance, comply this statement in a way that the expression of IL-6Rα is decreasing with the increase in 6-OHDA concentrations (Figure 3.13 and 3.14), with the exception for 6-OHDA concentration of 25 µM. The comparatively higher expression in 25 µM 6-OHDA concentration might be due to some experimental error or the cells could have produced the counter effect to overcome the decreased level of IL6 at higher 6OHDA concentration.

Notably, balanced production of pleiotropic cytokine, IL6 is essential since it has been proved to have the protective role (via STAT3 and ERK activation) in the neurodegenerative disease like PD, though it has some deleterious effect on CNS. But, the clear neuroprotective effect of IL6 is not raveled yet (Spooren et al., 2011). Since, as stated earlier that IL6 is neuroprotective in PD, we can believe that 6-OHDA likely hinders the regeneration of oxidatively stressed neuronal cells by inhibiting the secretion of neuroprotective IL6. However, it's quite difficult to interpret, with our data, the direct effect of oxidative stress generated by 6-OHDA on limitingly expressed IL-6Rα in a neuronal cell.

Our findings concerning the effect of 6-OHDA on alpha-synuclein tell us that the expression of alpha-synuclein is decreased in presence of 6-OHDA (Figure 3.13 and 3.14). This could be due to either lower production or higher turnover or less release, which is not clear. It has been revealed that endogenous proteasome activity (20S proteasome activity as well) is degraded by 6-OHDA in SHSY5Y cells leading to increased intracellular aggregation alpha-synuclein. Moreover, apart from the proteasomal activity, it is also proposed that the formation of o-o dityrosine by oxidative cross-linking of alpha-synuclein might contribute in stabilizing the aggregated oligomers which suggests the role of oxidative stress in intracellular accumulation of alpha-synuclein in neuronal cells (Souza, Giasson, Chen, Lee, & Ischiropoulos, 2000). So, from our study, we can assume that beside the proteasomal activity, the oxidative stress generated by 6-OHDA, could stabilize the alpha-synuclein in presence of 6-OHDA. But, it is difficult to interpret the mechanism behind the less expression of accumulated alpha-synuclein in presence of 6-OHDA.The higher expression of the alpha-synuclein in untreated cells (0 µM 6-OHDA) could be due to the higher production or less turnover or high release, which is not clear as well.

We can believe, based on our findings and the previous studies, that alpha-synuclein, a major protein in a neuron, gets abnormally aggregated with the oxidative stress eventually leading to the neurodegeneration. However, the exact mechanism remains largely unknown (Alves da Costa et al., 2006; Hashimoto et al., 1999; Souza et al., 2000). Not surprisingly, the alpha-synuclein, with increasing evidence, have been found to be abnormally accumulated in the neurodegenerative diseases like PD (Lashuel et al., 2013; Uversky, 2008).

5.CONCLUSION

We concluded with the two primary aspects in the neuronal cells SHSY5Y, concerning the neurodegenerative disease, PD. Firstly, the pure intact mitochondrial isolation from the neuroblastoma cells and secondly, the effect of neurotoxin 6-OHDA on the cell survival and their different proteins.

Various isolation and extraction methods were applied to isolate the mitochondria from SHSY5Y cells. The use of dounce homogenizer was found to be the most inspiring method and was pursued for the experiment. However, the grueling efforts had to be put on to improve the reproducibility of intact mitochondria. Our findings likely suggest that the dounce homogenization does not yield the intact mitochondria in a reproducible manner, which can possibly intervene with the thorough proteomics research.

6-OHDA, the firstly discovered well-recognized neurotoxin, has been proved to be cytotoxic to neuroblastoma cells suggesting its key role in the progression of neurodegenerative disease like PD. Although not fully understood, our result gives a hint that the 6-OHDA, which affects presumably via oxidative stress, can cause the neuronal cell death through different unknown mechanisms. The proteins like alpha-synuclein, IL-6Rα, TOM20 and MAP2 are affected by the underlying mechanism which could be the direct or indirect part of 6-OHDA action. However, the direct pronounced effect of this toxin to IL-6Rα pertinent with the neuroinflammation is difficult to elaborate. We believe, with the support of the accumulating evidence, 6-OHDA has profound effects on the mitochondrial import machinery TOM20, alpha-synuclein (major component of Lewy body in SN) and MAP2, a key protein in microtubule assembly. Many lines of scientific evidence have illustrated the deleterious role of 6-OHDA in the neurodegenerative disease, which we can also likely believe via our study, though the exact mechanism remains elusive. Herein, in our study, the expression level of different proteins in the neuronal cell SHSY5Y bestowed us with the influence of 6-OHDA on the cellular viability and possible detrimental effects of 6-OHDA. So, it would be further interesting to investigate and well characterize the change in protein morphology and its dynamic state in oxidatively stressed neuronal cells so that the underlying mechanism of neurodegeneration can be deciphered well.

6.FUTURE PERSPECTIVES

Many scientific protocols have described on the mitochondrial isolation from the cells using the most convenient method, homogenization. However, our findings suggest that the published methods, which we incorporated, were impossible or difficult to reproduce and we had to put grueling efforts to improve the situation for intact mitochondrial isolation. So, this suggests that the future work should involve the discovery of more optimized homogenization methods, that particularly, involves the automated process rather than the manual, to isolate the pure intact mitochondrial fractions from the cultured cells. This might eventually help in the intact mitochondrial isolation in a reproducible manner which is utmost to unveil the intricate mitochondrial dynamics in the neurodegenerative diseases.

To date, whatever have been proposed regarding the mechanism of neurotoxin 6-OHDA on the neuronal cell death remains rudimentary at the molecular level. Along with the several lines of evidence from the past, our understanding in the exact mechanism of 6-OHDA that affects the cell survival either via oxidative stress or the mitochondrial dysfunction is still not adequate to explore the exact pathogenetic mechanism of neuronal cell death in the neurodegenerative diseases. Future work must cover the underlying mechanism of 6-OHDA on both the defects in mitochondrial dynamics and the involvement of different proteins that can damage the cellular and mitochondrial functions at the molecular level.

Taken together, our data might provide the important implications for the future direction of the molecular study of the protein import machine TOM20, alpha-synuclein, MAP2 and the IL-6Rα since they were found likely to be affected by 6-OHDA. The very interesting point is to investigate the role of cytokines like IL6 and IL-6Rα which have been highly associated with the neuroinflammation in neurodegenerative diseases of whose only little is known about. Their further study at the molecular level is a must in upcoming days that can contribute in developing the potential therapeutic agents for the neurodegenerative diseases.

Importantly, alpha-synuclein, which has been proposed to have a significant role in the pathogenesis of neurodegenerative diseases since long, is needed to be addressed more at the molecular level, to unravel how the abnormal aggregation of this protein and its toxic nature affects the cellular pathway.

The profound study of the effect of presumably the oxidative stress on neuronal cells including the mitochondria at the precise level can likely contribute in developing the potential therapeutic agent for the neurodegenerative diseases like PD. The future work, in the neurodegenerative disease study, should entirely be based on the study of cellular pathways susceptible to oxidative stress produced by any extracellular stress or the endogenous-toxin like 6-OHDA. More importantly, various proteins in the neuronal cell can interplay in the progression of the neurodegenerative state. Hence, they need to be studied vastly to explore the neuropathogenesis.

REFERENCES

Abou-Sleiman, P. M., Muqit, M. M. K., & Wood, N. W. (2006). Expanding insights of mitochondrial dysfunction in Parkinson's disease. *Nature Reviews Neuroscience*, *7*(3), 207–219. https://doi.org/10.1038/nrn1868

Ahmed, S. T., & Ivashkiv, L. B. (2000). Inhibition of IL-6 and IL-10 signaling and Stat activation by inflammatory and stress pathways. *Journal of Immunology (Baltimore, Md. : 1950)*, *165*(9), 5227–37. Retrieved from http://www.ncbi.nlm.nih.gov/pubmed/11046056

Alves da Costa, C., Dunys, J., Brau, F., Wilk, S., Cappai, R., & Checler, F. (2006). 6-Hydroxydopamine but not 1-methyl-4-phenylpyridinium abolishes alpha-synuclein anti-apoptotic phenotype by inhibiting its proteasomal degradation and by promoting its aggregation. *The Journal of Biological Chemistry*, *281*(14), 9824–31. https://doi.org/10.1074/jbc.M513903200

Atreya, R., Finotto, S., Mudter, J., Mullberg, J., Jostock, T., Holtmann, M., … Neurath, M. F. (2000). Blockade of IL-6 transsignaling abrogates established experimental colitis in mice by suppression of T cell resistance against apoptosis. *Gastroenterology*, *118*(4), A863. https://doi.org/10.1016/S0016-5085(00)85593-6

Biedler, J., Helson, L., & Spengler, B. (1973). Morphology and growth, tumorigenicity, and cytogenetics of human neuroblastoma cells in continuous culture. *Cancer Research*. Retrieved from http://cancerres.aacrjournals.org/content/33/11/2643.short

Blum, D., Torch, S., Lambeng, N., & Nissou, M. (2001). Molecular pathways involved in the neurotoxicity of 6-OHDA, dopamine and MPTP: contribution to the apoptotic theory in Parkinson's disease. *Progress in*. Retrieved from http://www.sciencedirect.com/science/article/pii/S030100820100003X

Bonifati, V., Rizzu, P., Baren, M. van, & Schaap, O. (2003). Mutations in the DJ-1 gene associated with autosomal recessive early-onset parkinsonism. Retrieved from http://science.sciencemag.org/content/299/5604/256.short

Braak, H., Del Tredici, K., Rüb, U., de Vos, R. A. I., Jansen Steur, E. N. H., Braak, E., & al., et. (2000). Staging of brain pathology related to sporadic Parkinson's disease. *Neurobiology of Aging*, *24*(2), 197–211. https://doi.org/10.1016/S0197-4580(02)00065-9

Brand, M., Affourtit, C., Esteves, T., & Green, K. (2004). Mitochondrial superoxide: production, biological effects, and activation of uncoupling proteins. *Free Radical Biology*. Retrieved from http://www.sciencedirect.com/science/article/pii/S0891584904004538

Burden, D. (2008). Guide to the homogenization of biological samples. *Random Primers*. Retrieved from http://opsdiagnostics.com/notes/ranpri/Homogenization Guide ver.1.pdf

Chapter 2 Methods of cell breakage: assessing their suitability and efficacy. (1979) (pp. 11–44). https://doi.org/10.1016/S0075-7535(08)70462-5

Clarkson, E. D., Edwards-Prasad, J., Freed, C. R., & Prasad, K. N. (1999). Immortalized dopamine neurons: A model to study neurotoxicity and neuroprotection. *Proceedings of the Society for Experimental Biology and Medicine. Society for Experimental Biology and Medicine (New York, N.Y.)*, *222*(2), 157–63. Retrieved from http://www.ncbi.nlm.nih.gov/pubmed/10564540

Clayton, D. A., & Shadel, G. S. (n.d.). Isolation of Mitochondria from Cells and Tissues. https://doi.org/10.1101/pdb.top074542

Clayton, D. A., & Shadel, G. S. (2014). Isolation of mitochondria from tissue culture cells. *Cold Spring Harbor Protocols*, *2014*(10), pdb.prot080002. https://doi.org/10.1101/pdb.prot080002

Davies, K., & Daum, B. (2013). Role of cryo-ET in membrane bioenergetics research. Retrieved from http://www.biochemsoctrans.org/content/41/5/1227.abstract

de Araújo, M. E. G., Lamberti, G., & Huber, L. A. (2015). Homogenization of Mammalian Cells. *Cold Spring Harbor Protocols*, *2015*(11), 1009–12. https://doi.org/10.1101/pdb.prot083436

Dexter, D., & Jenner, P. (2013). Parkinson disease: from pathology to molecular disease mechanisms. *Free Radical Biology and Medicine*. Retrieved from http://www.sciencedirect.com/science/article/pii/S0891584913000282

Di Maio, R., Barrett, P. J., Hoffman, E. K., Barrett, C. W., Zharikov, A., Borah, A., … Greenamyre, J. T. (2016). α-Synuclein binds to TOM20 and inhibits mitochondrial protein import in Parkinson's disease. *Science Translational Medicine*, *8*(342), 342ra78. https://doi.org/10.1126/scitranslmed.aaf3634

Duty, S., & Jenner, P. (2011). Animal models of Parkinson's disease: a source of novel treatments and clues to the cause of the disease. *British Journal of Pharmacology*, *164*(4), 1357–91. https://doi.org/10.1111/j.1476-5381.2011.01426.x

Endo, T., & Kohda, D. (2002). Functions of outer membrane receptors in mitochondrial protein import. *Biochimica et Biophysica Acta (BBA) - Molecular Cell Research*, *1592*(1), 3–14. https://doi.org/10.1016/S0167-4889(02)00259-8

Falkenburger, B., & Saridaki, T. (2016). Cellular models for Parkinson's disease. *Of Neurochemistry*. Retrieved from http://onlinelibrary.wiley.com/doi/10.1111/jnc.13618/full

Farrer, M., Gwinn-Hardy, K., Muenter, M., DeVrieze, F. W., Crook, R., Perez-Tur, J., … Hardy, J. (1999). A chromosome 4p haplotype segregating with Parkinson's disease and postural tremor. *Human Molecular Genetics*, *8*(1), 81–5. https://doi.org/10.1093/HMG/8.1.81

Funayama, M., Hasegawa, K., Kowa, H., & Saito, M. (2002). A new locus for Parkinson's disease (PARK8) maps to chromosome 12p11. 2–q13. 1. *Annals of*. Retrieved from http://onlinelibrary.wiley.com/doi/10.1002/ana.10113/full

Gao, H.-M., & Hong, J.-S. (2011). Gene-environment interactions: key to unraveling the mystery of Parkinson's disease. *Progress in Neurobiology*, *94*(1), 1–19. https://doi.org/10.1016/j.pneurobio.2011.03.005

Gardiner, J., Overall, R., & Marc, J. (2013). The Nervous System Cytoskeleton under Oxidative Stress. *Diseases*. Retrieved from http://www.mdpi.com/2079-9721/1/1/36/html

Gasser, T. (2004). Genetics of Parkinson's disease. *Dialogues in Clinical Neuroscience*. Retrieved from http://pubmedcentralcanada.ca/pmcc/articles/PMC3181809/

Glinka, Y. Y., & Youdim, M. B. H. (1995). Inhibition of mitochondrial complexes I and IV by 6-hydroxydopamine. *European Journal of Pharmacology: Environmental Toxicology and Pharmacology*, *292*(3–4), 329–332. https://doi.org/10.1016/0926-6917(95)90040-3

Gomez-Lazaro, M., Bonekamp, N., & Galindo, M. (2008). 6-Hydroxydopamine (6-OHDA) induces Drp1-dependent mitochondrial fragmentation in SH-SY5Y cells. *Free Radical Biology*. Retrieved from http://www.sciencedirect.com/science/article/pii/S0891584908001524

Graham, J. (2002). Homogenization of mammalian cultured cells. *The Scientific World Journal*. Retrieved from https://www.hindawi.com/journals/tswj/2002/794041/abs/

Hald, A., & Lotharius, J. (2005). Oxidative stress and inflammation in Parkinson's disease: is there a causal link? *Experimental Neurology*, *193*(2), 279–290. https://doi.org/10.1016/j.expneurol.2005.01.013

Hashimoto, M., Hsu, L. J., Xia, Y., Takeda, A., Sisk, A., Sundsmo, M., & Masliah, E. (1999). Oxidative stress induces amyloid-like aggregate formation of NACP/alpha-synuclein in vitro. *Neuroreport*, *10*(4), 717–21. Retrieved from http://www.ncbi.nlm.nih.gov/pubmed/10208537

HEINRICH, P. C., BEHRMANN, I., HAAN, S., HERMANNS, H. M., MÜLLER-NEWEN, G., & SCHAPER, F. (2003). Principles of interleukin (IL)-6-type cytokine signalling and its regulation. *Biochemical Journal*, *374*(1). Retrieved from http://www.biochemj.org/content/374/1/1

Henchcliffe, C., & Beal, M. F. (2008). Mitochondrial biology and oxidative stress in Parkinson disease pathogenesis. *Nature Clinical Practice Neurology*, *4*(11), 600–609. https://doi.org/10.1038/ncpneuro0924

Hornykiewicz, O. (1998). Biochemical aspects of Parkinson's disease. *Neurology*. Retrieved from http://www.neurology.org/content/51/2_Suppl_2/S2.short

Iglesias-González, J., Sánchez-Iglesias, S., Méndez-Álvarez, E., Rose, S., Hikima, A., Jenner, P., & Soto-Otero, R. (2012). Differential Toxicity of 6-Hydroxydopamine in SH-SY5Y Human Neuroblastoma Cells and Rat Brain Mitochondria: Protective Role of Catalase and Superoxide Dismutase. *Neurochemical Research*, *37*(10), 2150–2160. https://doi.org/10.1007/s11064-012-0838-6

Jellinger, K., Linert, L., Kienzl, E., Herlinger, E., & Youdim, M. B. (1995). Chemical evidence for 6-hydroxydopamine to be an endogenous toxic factor in the pathogenesis of Parkinson's disease. *Journal of Neural Transmission. Supplementum*, *46*, 297–314. Retrieved from http://www.ncbi.nlm.nih.gov/pubmed/8821067

Jr, D. N. (1960). The isolation of a cell membrane fraction from rat liver. *Journal of Biophysical and Biochemical Cytology*. Retrieved from https://www.ncbi.nlm.nih.gov/pmc/articles/PMC2224936/

Kappler, L., Li, J., Häring, H.-U., Weigert, C., Lehmann, R., Xu, G., & Hoene, M. (2016a). Purity matters: A workflow for the valid high-resolution lipid profiling of mitochondria from cell culture samples. *Scientific Reports*, *6*(1), 21107. https://doi.org/10.1038/srep21107

Kappler, L., Li, J., Häring, H.-U., Weigert, C., Lehmann, R., Xu, G., & Hoene, M. (2016b). Purity matters: A workflow for the valid high-resolution lipid profiling of mitochondria from cell culture samples. *Scientific Reports*, *6*(1), 21107. https://doi.org/10.1038/srep21107

Kaur, N., Lu, B., Ward, S. M., & Halvorsen, S. W. (2005). Inducers of oxidative stress block ciliary neurotrophic factor activation of Jak/STAT signaling in neurons. *Journal of Neurochemistry*, *92*(6), 1521–1530. https://doi.org/10.1111/j.1471-4159.2004.02990.x

Kim, G. H., Kim, J. E., Rhie, S. J., & Yoon, S. (2015). The Role of Oxidative Stress in Neurodegenerative Diseases. *Experimental Neurobiology*, *24*(4), 325–40. https://doi.org/10.5607/en.2015.24.4.325

Kitada, T., Asakawa, S., Hattori, N., & Matsumine, H. (1998). Mutations in the parkin gene cause autosomal recessive juvenile parkinsonism. *Nature*. Retrieved from http://www.nature.com/nature/journal/v392/n6676/abs/392605a0.html

Kristian et al. (2006). Mitochondrial Purification via Percoll Gradient from Adherent Cells Grown In Culture. *Neuroscience*, *152*, 136–143. Retrieved from https://genome.duke.edu/sites/default/files/Purificationofmitochondria_MMihovilovic_4May2011_0.pdf

Kroemer, G., Dallaporta, B., & Resche-Rigon, M. (1998). THE MITOCHONDRIAL DEATH/LIFE REGULATOR IN APOPTOSIS AND NECROSIS. *Annual Review of Physiology*, *60*(1), 619–642. https://doi.org/10.1146/annurev.physiol.60.1.619

Kühlbrandt, W. (2015). Structure and function of mitochondrial membrane protein complexes. *BMC Biology*. Retrieved from https://bmcbiol.biomedcentral.com/articles/10.1186/s12915-015-0201-x

Lashuel, H., Overk, C., & Oueslati, A. (2013). The many faces of α-synuclein: from structure and toxicity to therapeutic target. *Nature Reviews*. Retrieved from http://www.nature.com/nrn/journal/v14/n1/abs/nrn3406.html

Lau, L. De, & Breteler, M. (2006). Epidemiology of Parkinson's disease. *The Lancet Neurology*. Retrieved from http://www.sciencedirect.com/science/article/pii/S1474442206704719

Leroy, E., Boyer, R., Auburger, G., Leube, B., & Ulm, G. (1998). The ubiquitin pathway in Parkinson's disease. *Nature*. Retrieved from http://www.nature.com/nature/journal/v395/n6701/abs/395451a0.html

Levites, Y., Youdim, M. B. H., Maor, G., & Mandel, S. (2002). Attenuation of 6-hydroxydopamine (6-OHDA)-induced nuclear factor-kappaB (NF-κB) activation and cell death by tea extracts in neuronal cultures. *Biochemical Pharmacology*, *63*(1), 21–29. https://doi.org/10.1016/S0006-2952(01)00813-9

Lin, M., & Beal, M. (2006). Mitochondrial dysfunction and oxidative stress in neurodegenerative diseases. *Nature*. Retrieved from http://www.nature.com/nature/journal/v443/n7113/abs/nature05292.html

Liu, Y., Fiskum, G., & Schubert, D. (2002). Generation of reactive oxygen species by the mitochondrial electron transport chain. *Journal of Neurochemistry*. Retrieved from http://onlinelibrary.wiley.com/doi/10.1046/j.0022-3042.2002.00744.x/full

Lodish, H., Berk, A., Zipursky, S. L., Matsudaira, P., Baltimore, D., & Darnell, J. (2000). Purification of Cells and Their Parts. Retrieved from https://www.ncbi.nlm.nih.gov/books/NBK21492/

Lotharius, J., & Brundin, P. (2002). Pathogenesis of Parkinson's disease: dopamine, vesicles and α-synuclein. *Nature Reviews Neuroscience*. Retrieved from http://www.nature.com/nrn/journal/v3/n12/abs/nrn983.html

Lotharius, J., Dugan, L., & O'malley, K. (1999). Distinct mechanisms underlie neurotoxin-mediated cell death in cultured dopaminergic neurons. *Journal of Neuroscience*. Retrieved from http://www.jneurosci.org/content/19/4/1284.short

Michel, P., & Hefti, F. (1990). Toxicity of 6-hydroxydopamine and dopamine for dopaminergic neurons in culture. *Journal of Neuroscience Research*. Retrieved from http://onlinelibrary.wiley.com/doi/10.1002/jnr.490260405/full

Monte, D. Di, Lavasani, M., & Manning-Bog, A. (2002). Environmental factors in Parkinson's disease. *Neurotoxicology*. Retrieved from http://www.sciencedirect.com/science/article/pii/S0161813X02000992

Mouradian, M. (2002). Recent advances in the genetics and pathogenesis of Parkinson disease. *Neurology*. Retrieved from http://www.neurology.org/content/58/2/179.short

Müller, T. (2012). Drug therapy in patients with Parkinson's disease. *Translational Neurodegeneration*. Retrieved from https://translationalneurodegeneration.biomedcentral.com/articles/10.1186/2047-9158-1-10

Murray, R., & Kincaid, R. (2012). *Harper's illustrated biochemistry*. Retrieved from http://dl.kums.ac.ir/handle/Hannan/5886

Napolitano, A., Crescenzi, O., & Pezzella, A. (1995). Generation of the Neurotoxin 6-Hydroxydopamine by Peroxidase/H~ 2O~ 2 Oxidation of Dopamine. *Journal of Medicinal*. Retrieved from http://wpage.unina.it/apezzell/SitoCUN/JMC - dopamine H2O2 - 1995.pdf

Patel, V. P., & Chu, C. T. (2014). Decreased SIRT2 activity leads to altered microtubule dynamics in oxidatively-stressed neuronal cells: implications for Parkinson's disease. *Experimental Neurology*, *257*, 170–81. https://doi.org/10.1016/j.expneurol.2014.04.024

Perier, C., & Vila, M. (2012). Mitochondrial biology and Parkinson's disease. *Spring Harbor Perspectives in* …. Retrieved from http://perspectivesinmedicine.cshlp.org/content/2/2/a009332.short

Polymeropoulos, M., Lavedan, C., Leroy, E., & Ide, S. (1997). Mutation in the α-synuclein gene identified in families with Parkinson's disease. Retrieved from http://science.sciencemag.org/content/276/5321/2045.short

Przedborski, S., & Ischiropoulos, H. (2005). Reactive oxygen and nitrogen species: weapons of neuronal destruction in models of Parkinson's disease. *Antioxidants & Redox*. Retrieved from http://online.liebertpub.com/doi/abs/10.1089/ars.2005.7.685

Rakovic, A., Shurkewitsch, K., Seibler, P., Grunewald, A., Zanon, A., Hagenah, J., … Klein, C. (2013). Phosphatase and Tensin Homolog (PTEN)-induced Putative Kinase 1 (PINK1)-dependent Ubiquitination of Endogenous Parkin Attenuates Mitophagy: STUDY IN HUMAN PRIMARY FIBROBLASTS AND INDUCED PLURIPOTENT STEM CELL-DERIVED NEURONS. *Journal of Biological Chemistry*, *288*(4), 2223–2237. https://doi.org/10.1074/jbc.M112.391680

Reisinger, V., & Eichacker, L. A. (2006). Analysis of Membrane Protein Complexes by Blue Native PAGE. *PROTEOMICS*, *6*(S2), 6–15. https://doi.org/10.1002/pmic.200600553

Riederer, P., Sofic, E., & Rausch, W. (1989). Transition metals, ferritin, glutathione, and ascorbic acid in parkinsonian brains. *Journal of*. Retrieved from http://onlinelibrary.wiley.com/doi/10.1111/j.1471-4159.1989.tb09150.x/full

Ryu, M., & Nakazawa, T. (2014). Calcium and Calpain Activation. In *Neuroprotection and Neuroregeneration for Retinal Diseases* (pp. 13–24). Tokyo: Springer Japan. https://doi.org/10.1007/978-4-431-54965-9_2

Sánchez, C., Díaz-Nido, J., & Avila, J. (2000). Phosphorylation of microtubule-associated protein 2 (MAP2) and its relevance for the regulation of the neuronal cytoskeleton function. *Progress in Neurobiology*, *61*(2), 133–68. Retrieved from http://www.ncbi.nlm.nih.gov/pubmed/10704996

Sazanov, L. (2015). A giant molecular proton pump: structure and mechanism of respiratory complex I. *Nature Reviews Molecular Cell Biology*. Retrieved from http://www.nature.com/nrm/journal/v16/n6/abs/nrm3997.html

Schapira, A. (2007). Mitochondrial dysfunction in Parkinson's disease. *Cell Death and Differentiation*. Retrieved from http://search.proquest.com/openview/b14d658f65236313f2d23d33dad4bf57/1?pq-origsite=gscholar&cbl=44124

Schapira, A. (2008). Progress in Parkinson's disease. *European Journal of Neurology*. Retrieved from http://onlinelibrary.wiley.com/doi/10.1111/j.1468-1331.2007.02036.x/abstract

Schober, A. (2004). Classic toxin-induced animal models of Parkinson's disease: 6-OHDA and MPTP. *Cell and Tissue Research*. Retrieved from http://link.springer.com/article/10.1007/s00441-004-0938-y

Simola, N., Morelli, M., & Carta, A. (2007). The 6-hydroxydopamine model of Parkinson's disease. *Neurotoxicity Research*. Retrieved from http://link.springer.com/article/10.1007/BF03033565

Smith, J., Das, A., Ray, S., & Banik, N. (2012). Role of pro-inflammatory cytokines released from microglia in neurodegenerative diseases. *Brain Research Bulletin*. Retrieved from http://www.sciencedirect.com/science/article/pii/S0361923011002991

Smith, P., Krohn, R., Hermanson, G., & Mallia, A. (1985). Measurement of protein using bicinchoninic acid. *Analytical*. Retrieved from http://www.sciencedirect.com/science/article/pii/0003269785904427

Song, J.-X., Shaw, P.-C., Sze, C.-W., Tong, Y., Yao, X.-S., Ng, T.-B., & Zhang, Y.-B. (2010). Chrysotoxine, a novel bibenzyl compound, inhibits 6-hydroxydopamine induced apoptosis in SH-SY5Y cells via mitochondria protection and NF-κB modulation. *Neurochemistry International*, *57*(6), 676–689. https://doi.org/10.1016/j.neuint.2010.08.007

Souza, J. M., Giasson, B. I., Chen, Q., Lee, V. M., & Ischiropoulos, H. (2000). Dityrosine Cross-linking Promotes Formation of Stable alpha -Synuclein Polymers. IMPLICATION OF NITRATIVE AND OXIDATIVE STRESS IN THE PATHOGENESIS OF NEURODEGENERATIVE SYNUCLEINOPATHIES. *Journal of Biological Chemistry*, *275*(24), 18344–18349. https://doi.org/10.1074/jbc.M000206200

Spooren, A., Kolmus, K., Laureys, G., Clinckers, R., De Keyser, J., Haegeman, G., & Gerlo, S. (2011). Interleukin-6, a mental cytokine. *Brain Research Reviews*, *67*(1), 157–183. https://doi.org/10.1016/j.brainresrev.2011.01.002

Steece-Collier, K., Maries, E., & Kordower, J. H. (2002). Etiology of Parkinson's disease: Genetics and environment revisited. *Proceedings of the National Academy of Sciences of the United States of America*, *99*(22), 13972–4. https://doi.org/10.1073/pnas.242594999

Sun, X., Sun, X., Shi, X., Shi, X., Lu, L., Lu, L., … Liu, B. (2016). *Molecular medicine reports. Molecular Medicine Reports* (Vol. 13). D.A. Spandidos. Retrieved from https://www.spandidos-publications.com/mmr/13/3/2215?text=fulltext

Tieu, K. (2011). A guide to neurotoxic animal models of Parkinson's disease. *Spring Harbor Perspectives in Medicine*. Retrieved from http://perspectivesinmedicine.cshlp.org/content/1/1/a009316.short

Tsunoda, M. (2006). Recent advances in methods for the analysis of catecholamines and their metabolites. *Analytical and Bioanalytical Chemistry*, *386*(3), 506–514. https://doi.org/10.1007/s00216-006-0675-z

Uversky, V. N. (2008). Alpha-synuclein misfolding and neurodegenerative diseases. *Current Protein & Peptide Science*, *9*(5), 507–40. Retrieved from http://www.ncbi.nlm.nih.gov/pubmed/18855701

Wang, L., Xu, S., Xu, X., & Chan, P. (2009). (-)-Epigallocatechin-3-Gallate Protects SH-SY5Y Cells Against 6-OHDA-Induced Cell Death through STAT3 Activation. *Journal of Alzheimer's Disease*, *17*(2), 295–304. https://doi.org/10.3233/JAD-2009-1048

Wang, S.-W., & Sun, Y.-M. (2014). *International journal of oncology. International Journal of Oncology* (Vol. 44). University of Crete, Faculty of Medicine, Laboratory of Clinical Virology. Retrieved from https://www.spandidos-publications.com/10.3892/ijo.2014.2259

Wang, Y.-H., Xuan, Z.-H., Tian, S., & Du, G.-H. (2015). Echinacoside Protects against 6-Hydroxydopamine-Induced Mitochondrial Dysfunction and Inflammatory Responses in PC12 Cells via Reducing ROS Production. *Evidence-Based Complementary and Alternative Medicine, 2015*, 1–9. https://doi.org/10.1155/2015/189239

Warner, T., & Schapira, A. (2003). Genetic and environmental factors in the cause of Parkinson's disease. *Annals of Neurology*. Retrieved from http://onlinelibrary.wiley.com/doi/10.1002/ana.10487/full

Wettmarshausen, J., & Perocchi, F. (2017). Isolation of Functional Mitochondria from Cultured Cells and Mouse Tissues (pp. 15–32). https://doi.org/10.1007/978-1-4939-6824-4_2

Wieckowski, M. R., Giorgi, C., Lebiedzinska, M., Duszynski, J., & Pinton, P. (2009). Isolation of mitochondria-associated membranes and mitochondria from animal tissues and cells. *Nature Protocols*, *4*(11), 1582–1590. https://doi.org/10.1038/nprot.2009.151

Wood-Kaczmar, A., Gandhi, S., & Wood, N. (2006). Understanding the molecular causes of Parkinson's disease. *Trends in Molecular Medicine*. Retrieved from http://www.sciencedirect.com/science/article/pii/S147149140600219X

Xie, H., Hu, L., & Li, G. (2010). SH-SY5Y human neuroblastoma cell line: in vitro cell model of dopaminergic neurons in Parkinson's disease. *Chinese Medical Journal*. Retrieved from http://europepmc.org/abstract/med/20497720

Zhu, Y., Chen, G., Chen, L., Zhang, W., Feng, D., Liu, L., & Chen, Q. (2014). Monitoring Mitophagy in Mammalian Cells (pp. 39–55). https://doi.org/10.1016/B978-0-12-801415-8.00003-5

APPENDIX A

Curve Name	Curve Formula	A	B	C	D	R2	Fit F Prob
StdCurve	Y = (A-D)/(1+(X/C)^B) + D	0.0785	0.896	4.61E+04	38.7	0.997	?????
Curve Name	Curve Formula	Parameter	Value	Std. Error	95% CI min	95% CI max	Fit F Prob
StdCurve	Y = (A-D)/(1+(X/C)^B) + D	A	0.0785	0.105	-0.212	0.369	?????
		B	0.896	0.122	0.558	1.23	
		C	4.61E+04	7.67E+04	-1.67E+05	2.59E+05	
		D	38.7	69.7	-155	232	

	1	2	3	4	5	6	7	8	9	10	11	12
A	2.312	1.709	1.278	1.047	0.775	0.431	0.269	0.108	0.073	0.084	0.079	0.074
B	0.165	0.125	0.098	0.085	0.084	0.083	0.167	0.121	0.109	0.441	0.335	0.201
C	0.239	0.147	0.113	0.54	0.317	0.207	0.725	0.421	0.185	0.505	0.332	0.108
D	0.36	0.209	0.14	0.517	0.326	0.18	0.408	0.27	0.167			
E												

Well ID	Well ID	Name	Well	Conc/Dil	562	[Concentration] x Dil
BLK	BLK		A9		0.073	
SPL1	SPL1		A10	1	0.084	2.426
			A11	2	0.079	0.371

			A12	4	0.074	<0,000
SPL2	SPL2		B1	1	0.165	50.655
			B2	2	0.125	50.862
			B3	4	0.098	37.83
SPL3	SPL3		B4	1	0.085	2.957
			B5	2	0.084	4.377
			B6	4	0.083	6.7
SPL4	SPL4		B7	1	0.167	52.436
			B8	2	0.121	45.632
			B9	4	0.109	62.78
SPL5	SPL5		B10	1	0.441	254.34
			B11	2	0.335	343.618
			B12	4	0.201	300.128
SPL6	SPL6		C1	1	0.239	101.957
			C2	2	0.147	78.569
			C3	4	0.113	71.677
SPL7	SPL7		C4	1	0.54	333.417
			C5	2	0.317	316.895
			C6	4	0.207	317.22
SPL8	SPL8		C7	1	0.725	489.057
			C8	2	0.421	476.42
			C9	4	0.185	255.712
SPL9	SPL9		C10	1	0.505	305.476
			C11	2	0.332	339.247
			C12	4	0.108	62.083
SPL10	SPL10		D1	1	0.36	191.313

			D2	2	0.209	161.101
			D3	4	0.14	139.821
SPL11	SPL11		D4	1	0.517	314.701
			D5	2	0.326	331.126
			D6	4	0.18	244.129
SPL12	SPL12		D7	1	0.408	228.049
			D8	2	0.27	248.486
			D9	4	0.167	209.479
STD1	STD1		A1	2000	2.312	
STD2	STD2		A2	1500	1.709	
STD3	STD3		A3	1000	1.278	
STD4	STD4		A4	750	1.047	
STD5	STD5		A5	500	0.775	
STD6	STD6		A6	250	0.431	
STD7	STD7		A7	125	0.269	
STD8	STD8		A8	25	0.108	

Plot of BSA protein standards vs the absorbance at λ=562 nm

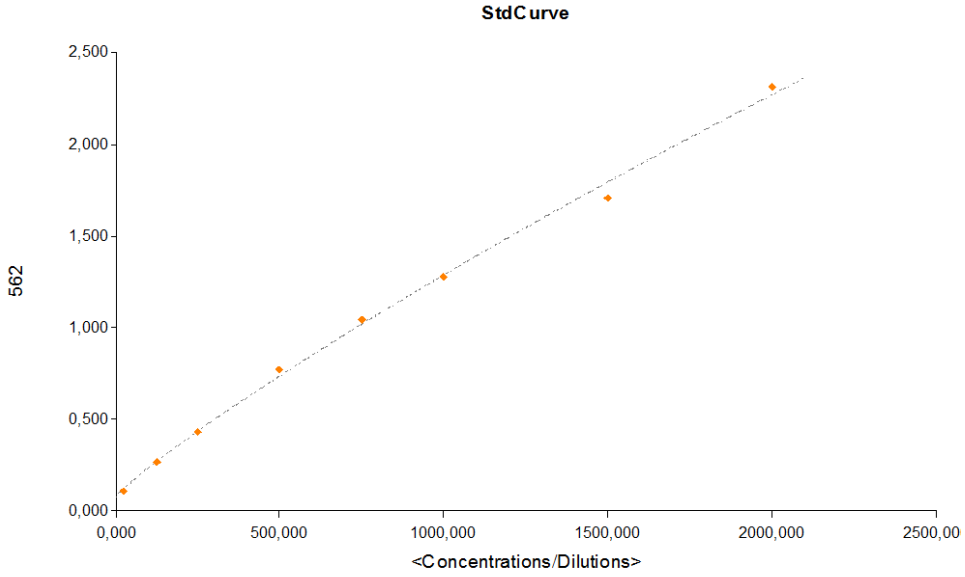

APPENDIX B

	Expt 1	Expt 2	Expt 3	Expt 4	Mean	CV	SD
6-OHDA conc. µM	**%**	**%**	**%**	**%**	**%**	**%**	
0	100	100	100	100	100	0	0
2.5	107	100	100	115	105	6.8	7.1
5	114	107	113	125	115	6.5	7.5
10	112	104	114	100	108	6.2	6.7
25	119	52	108	89	92	32.0	29.5
50	34	39	49	117	60	64.9	38.7
100	27	26	31	33	29	11.2	3.3
250	31	23	36	37	32	20.0	6.4

500	38	32	48	45	41	17.6	7.2

APPENDIX C

Coomassie staining solution (for 1000ml water)

0.02%(w/v) CBB G-250 - 0.2g

5%(w/v) Aluminium sulfate (14-18)-hydrate- 50g

10%(w/v) ethanol (96%) -100ml

2%(w/v) Orthophosphoric acid (85%) -23.5 ml

APPENDIX D

Mowiol 4-88 preparation

1.Mix the mixture of 2.4g of Mowiol 4-88 and 6g glycerol.

2.Add 6ml of water to above mixture.

3.Add 12 ml of 0.2M Tris Cl pH 8.5.

4.Stirr the solution and heat it to 50°C for about 3 hr.

5.Centrifuge at 5000g for 15 min.

6.Add 2.5% DABCO and store at -20°C.